NASA CONTRACTOR REPORT

RADIATION DAMAGE IN SILICON

Prepared by: N. ALMELEH, B. GOLDSTEIN (Project Engineer), and J. J. WYSOCKI

Approved by: P. RAPPAPORT (Project Supervisor)

FINAL REPORT

For the Period

OCTOBER 15, 1963 to OCTOBER 15, 1964

Prepared under Contract No. NAS 5-3788

RADIO CORPORATION OF AMERICA
RCA LABORATORIES
PRINCETON, NEW JERSEY

for

NATIONAL AERONAUTICS & SPACE ADMINISTRATION • WASHINGTON, D. C. • [illegible]ER 1964
GODDARD SPACE FLIGHT CENTER

FOREWORD

The work reported in this Final Report covers the period October 15, 1963 to November 30, 1964. We would like to acknowledge the helpful discussions and guidance of Mr. Milton Schach and Dr. Paul Fang (Project Monitor) of NASA Goddard Space Flight Center during the course of this work.

The work reported herein has ranged from the basic research on radiation-induced defects in silicon to the behavior of solar cells in proton and electron environments. It is felt that the approach we have taken in this work will contribute significantly to the understanding and control of radiation damage effects in solar cells. The electron spin resonance work has reached the point where it is beginning to pay off in terms of the correlation of electron paramagnetic resonance properties with electrical properties of silicon, especially the resistivity. This should help in developing a physical model of the damage center.

The interaction of lithium with radiation-induced defects has proven to be quite interesting. Lithium is the first metallic impurity with which we could affect damage properties in silicon. Further work in this area should prove exciting.

ABSTRACT

19693

Electron paramagnetic resonance (EPR) studies have been made of the dominant paramagnetic defect produced in p-type silicon when bombarded by electrons at energies from 1 MeV to 6.6 MeV. The principal axes of this defect are along the <221>, <1$\bar{1}$0>, and <11$\bar{4}$> directions. The g-values along these directions are 2.0000, 2.0066, and 2.0056, respectively. The introduction rates have been measured to be 0.03 cm^{-1} and 0.15 cm^{-1} at 1 MeV and 6.6 MeV, respectively. The electronic level corresponding to this defect is between the valence band edge and 0.3 eV above it. The symmetry axis, <221>, suggests that the defect involves a substitutional oxygen atom in association with a next-nearest neighbor silicon interstitial. EPR measurements are being correlated with the electrical properties of silicon for the first time.

Diffusion length measurements have been used to study the effects of impurities on radiation damage in silicon produced by electron bombardment. Aluminum, boron, gallium, indium, and gadolinium produce equal radiation damage resistance when they are used in solar cells with a base resistivity of 1 to 10 Ω-cm. The radiation resistance of lithium n-on-p cells is greater than that of phosphorus n-on-p cells although the deeper junctions of the lithium cells becloud this result somewhat. The diffusion of lithium throughout n-type silicon reduces its resistivity, yet the radiation damage resistance of surface barrier cells made from this material is typical of the predIffused material. Of all the impurities studied to date, only lithium has been found to give new and promising results.

The interaction between lithium and radiation-induced defects in silicon has been measured through the use of electron paramagnetic resonance. Simultaneous measurements of both the lithium resonance and the damage resonance have been made as functions of the lithium content and the bombarding electron flux at 6 MeV. It has been found that an increase in one invariably produces a concomitant decrease in the other. If lithium is introduced at 300°C, its resonance is completely removed by an electron flux of 2×10^{16} el/cm^2, while lithium introduced at 350°C completely removes any damage resonance with fluxes up to 2×10^{17} el/cm^2. Whether the interaction involves the complexing of lithium with a damage center or merely the supplying of a donor electron from lithium to the damage center is not clear. For a clarification of this point, electron bombardments at much lower energies, about 1 MeV, are required.

AUTHOR

TABLE OF CONTENTS

LIST OF ILLUSTRATIONS

I. ELECTRON PARAMAGNETIC RESONANCE STUDIES

A. INTRODUCTION

Electron paramagnetic resonance (EPR) has been used extensively in the past in the study of electrically active chemical impurities in semiconductors. It has been particularly useful in discerning the nature of the local environment of the paramagnetic center, the position occupied in the lattice, the identification of the charge state, the interactions with other chemical entities present in semiconductors, and in the structure of donor states.

The first studies of radiation damage centers were carried out by Bemski[1] and Watkins et al.[2] in electron-irradiated n-type silicon. The dominant center which appears in pulled n-type silicon, the A-center, was thoroughly studied by Watkins and Corbett.[3] They showed that the defect was connected with oxygen impurities present in the crystal. According to their model, an interstitial oxygen atom combines with a vacancy created by electron irradiation to produce a substitutional oxygen. This defect produces a net acceptor level 0.17 eV below the conduction band. In order for the spin resonance of this center to be observable, the temperature must be sufficiently low so that electrons from the donor atom can drop down to the defect level.

The initial work of Watkins and Corbett demonstrated the importance of impurities in the formation of damage centers which are stable at room temperature. They found that for floating-zone silicon, which contains less oxygen than pulled silicon ($\sim 10^{16}$ cm^{-3} and 10^{18} cm^{-3}, respectively), the A-center did not appear. A new center which they called the silicon E-center is created and is identified as arising from a donor atom-vacancy combination. They also identified a third defect which does not depend on impurities present in the crystal. This is the divacancy (Si C- and Si J-center), a stable combination of two vacancies. The silicon J-center and silicon C-center are considered to be the same defect center with different charge states, the former being detected in p-type silicon. At room temperature, the density of these defects is only 5% of the silicon A-center defects in pulled n-type silicon.

Recently, Watkins[5] identified a variety of damage centers and investigated the kinetics and nature of the motions of defects. Most of this work was accomplished at low temperatures in which the kinetics were followed through the changes in EPR spectra attending changes in temperature.

Our interest in spin resonance experiments of damage centers has been primarily to complement the measurements of the macroscopic properties of irradiated silicon. Much that has been learned about damage defects has been obtained from such measurements as resistivity, minority carrier lifetime, and optical absorption. The combination of electron spin resonance with these experimental methods is the approach considered here to provide information concerning the characterization and physical nature of radiation damage centers. For this reason, we have focused

our attention on the dominant paramagnetic defect center produced in low-resistivity ($\sim$ 2 Ω-cm) p-type silicon which has been irradiated at room temperature.

B. APPARATUS

The nature of EPR resonance of radiation-produced defects requires the use of a high-sensitivity spectrometer. To observe the silicon A-center, electrons must be supplied by the donor atoms. Thus, the maximum observable number of A-centers is equal to the number of donor atoms. For 1-Ω-cm silicon this is $N_D = 5 \times 10^{15}/cm^3$. The amount of silicon material used is limited by reasonable radiation times and the perturbation of the silicon on the microwave cavity. A typical volume used in this work is 0.1 cm^3. Therefore, the number of defect centers is 5×10^{14}.

The sensitivity of EPR spectrometers is usually specified as the minimum detectable number of spins observable at room temperature using the maximum or most favorable microwave power. Under these conditions our spectrometer using homodyne operation and a magnetic field modulation frequency of 400 cps has a sensitivity such that

$$N_{min} = 2 \times 10^{12} \Delta H \qquad (1)$$

where N_{min} = minimum detectable number of spins for a SNR = 1, and a filter time constant of 3 seconds.

ΔH = linewidth in gauss.

The value in Eq. (1) was determined by measuring the signal-to-noise ratio of the resonance from a small ruby crystal with a known Cr concentration.

When the spectrometer is used to study radiation damage defects the sensitivity is reduced in several ways. In general, lower power levels must be used because of saturation effects. Furthermore, the magnitude of the susceptibility signal depends on external experimental parameters, such as magnitude and frequency of magnetic field modulation and rate of magnetic field sweep, and it is not always possible to operate under conditions where the susceptibility signal is maximum.

To increase the sensitivity, a superheterodyne system had been added to the spectrometer, thus allowing operation at low power levels while still maintaining good sensitivity. This also reduced the crystal noise reaching the detection amplifier. However, the sensitivity obtainable in practice using the superheterodyne system usually falls below its theoretical value. The problem seems to be noise due to vibrations in the system.

In studying the symmetry properties of the paramagnetic damage center, the microwave bridge was arranged as shown in Fig. 1. This arrangement allows for the power in the reference

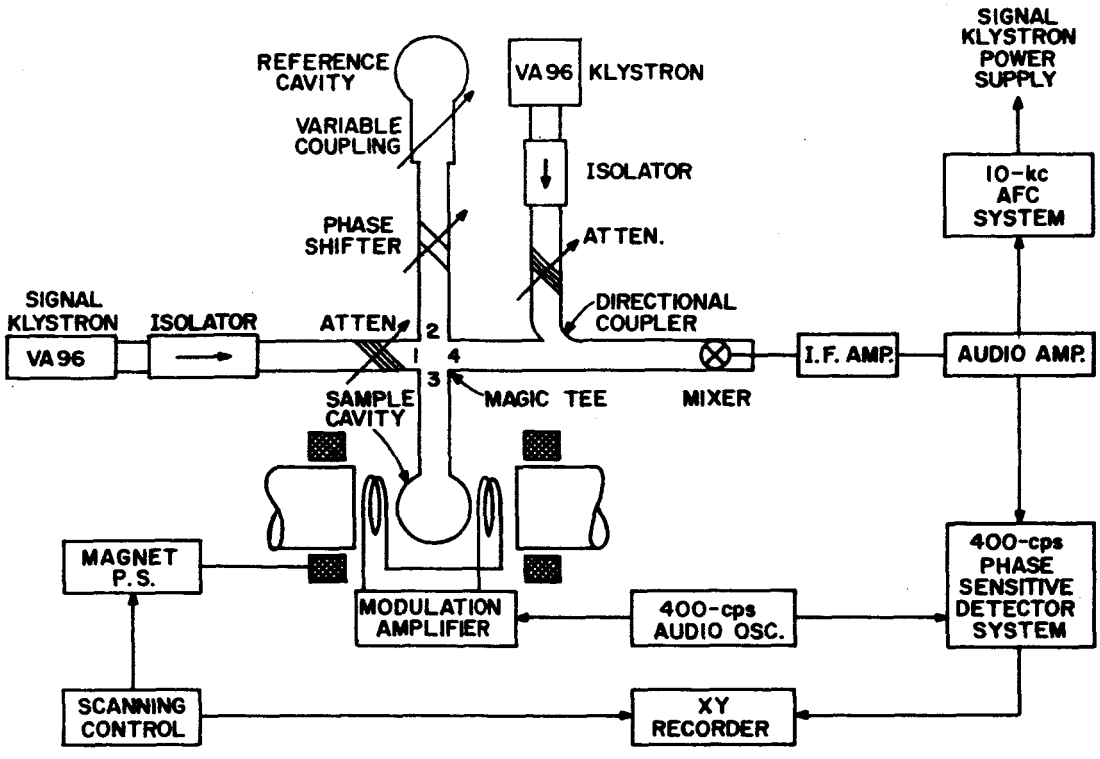

Fig. 1. K-band microwave bridge.

cavity and sample cavity to be balanced. When the balance is disturbed by moving the sample through resonance a signal appears in the fourth arm of the bridge. The signal is mixed with that of the local oscillator and picked up by the crystal detector. This system is sufficiently flexible so that the noise accruing from the klystron and crystal detector can be kept to low levels, especially the noise generated by the klystron at the higher power levels. In this setup, the klystron frequency is locked to the resonant frequency of the sample cavity, and the desired mode is selected by adjusting the phase of the signal reflected from the sample cavity with respect to the phase of the bias signal with a phase-shifter. But because the power is fed equally into both cavities, changing the phase also changes the coupling of the cavities to the bridge, thus requiring further adjustments in the other arms. This interaction results in a condition where the klystron may now be locked to the resonant frequency of either cavity, making it difficult to select exactly, if one so desired, a particular mode of operation of the bridge. In the measurement of the angular variation of the damage defect, this is of no great consequence. Considerations of sensitivity, however, are of greater concern.

On the other hand, in determining absolute spin densities it is imperative to have the spectrometer operating in the dispersion mode only. Experimentally and theoretically, it has been found that paramagnetic damage centers "saturate" more readily in the absorption mode.[6] As a consequence, the intensity of the resonance signal can vary appreciably in going from absorption modes to dispersion modes. One obtains maximum signal in the dispersion mode. Obviously, then,

the measurement of spin densities by comparison of the defect spectrum to a standard resonance signal requires that the bridge be operated strictly in the dispersion mode. To do this easily the phase-shifter was taken from the reference arm of the bridge as shown in Fig. 1, and placed in the sample arm together with a precision attenuator. This rearrangement accomplished two things. First, the power going into the sample cavity was decreased by 10 db with respect to the reference cavity thereby permitting the unequivocal fixing of the klystron to the latter resonant frequency. This, in essence, also isolated the sample arm from the rest of the bridge. Secondly, the phase of the reflected signal can be adjusted simply to the desired mode by using only the phase-shifter. The ease with which one can select the dispersion mode, however, was paid for at the price of a reduction in sensitivity by a factor of about two.

C. SPECIAL PROBLEMS IN STUDYING DAMAGE CENTERS

In trying to obtain the absolute density of defects from spin resonance measurements care must be taken to avoid errors arising from saturation of these lines. Saturation effects occur when the spin-lattice interaction is very weak and the relaxation times are therefore very long (of the order of seconds). The long spin-lattice relaxation time does not allow the electrons excited to the higher energy state to lose energy fast enough and drop back into the lower energy state. As a result, the population of these levels becomes equal, preventing the further absorption of radiation. Experimentally, this condition is observed by an apparent decrease in the relative size of the resonance signal and usually attended by an increase in linewidth.

The details of the saturation behavior of a system depend markedly on the nature of the line-broadening mechanism.[6,7] If broadening arises from dipolar interaction between like spins or from interaction with the radiation field, then the thermal equilibrium of the spin system will be preserved during resonance absorption. This will also be true if the linewidth comes from some mechanism which is external to the spin system but is fluctuating rapidly compared with the time associated with a spin transition. This case is known as the homogeneously broadened case. The consequence of homogeneous broadening is that the energy absorbed from the microwave field is distributed to all the spins, and thermal equilibrium of the spin system is maintained through resonance.

In the other case, known as the inhomogeneously broadened case, energy is transferred only to those spins whose local fields satisfy the resonance condition. Further, the processes for spin-spin interaction will be slow as compared with the direct interactions with the lattice since, for spins in different local fields to come to equilibrium, energy will have to be transferred to the lattice. The overall response of the spin system will therefore be a superposition of the individual responses of the spin packets.

It is this latter case with which we are concerned here. The resonance signal of inhomogeneously broadened lines is susceptible to changes in magnitude and shape depending on

experimental conditions other than microwave power. In particular, it has been found to be dependent upon how rapidly the conditions of excitation change as compared to the relaxation time of the spin system. These effects, known as passage effects, are peculiar to inhomogeneously broadened lines and have been investigated by Portis[6] and Weger.[7] Generally, passage effects depend in a complex manner on microwave field, magnetic field sweep rate, modulation field, modulation frequency, and the relaxation time of the system. Weger, in fact, has analyzed and confirmed experimentally the details of resonance lines expected for the limiting cases under eleven different passage conditions. An understanding of a part of this problem can be seen in Fig. 2 in which the intensity of the dispersion resonance is plotted against sweep field, microwave field, and modulation field. It is clear from this figure that if one is interested in making absolute measurements of spin concentrations from inhomogeneously broadened resonances one must know where on each of the three curves in Fig. 2 he is performing the spin resonance measurement.

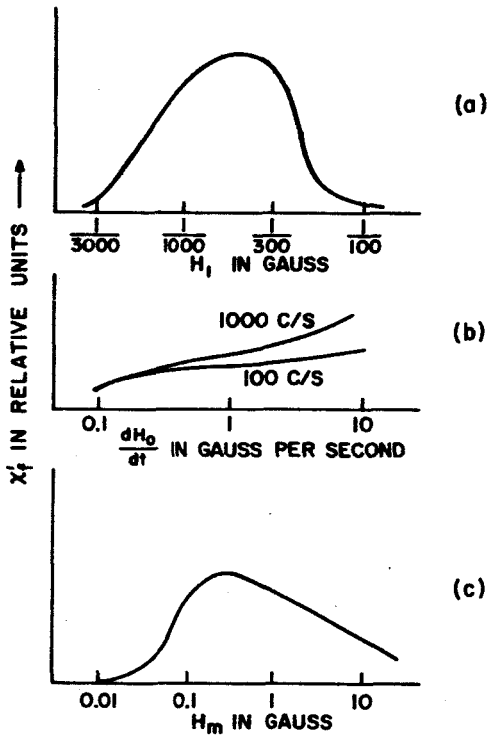

Fig. 2. Dependence of amplitude of dispersion signal (χ_f') upon (a) r-f magnetic field, H_1, (b) sweep field rate $\frac{dH_0}{dt}$ and (c) modulation amplitude H_m – according to Weger.

We have taken the time to emphasize some of the difficulties encountered with inhomogeneously broadened lines because the paramagnetic defect center, the K-center, belongs to this group of saturated resonances. The evidence for so classifying the K-center comes from the fact that the resonance does not change shape upon saturation nor do the observed line shape and

linewidth. This type of resonance behavior is characteristic of the other paramagnetic damage centers observed in silicon.[8]

D. CALIBRATION OF STANDARD SAMPLE

The determination of the absolute intensity of an electron resonance signal can, in principle, be affected by the use of the theoretical expressions for the change in detected power of the spectrometer. Such an absolute determination of spin densities, however, is seldom made in practice, and a comparison method employing a standard sample is generally adopted. For the best result the standard comparison sample should have a linewidth and intensity of the same order as those of the spectral lines to be measured.

In determining the absolute spin density of the K-center, the silicon conduction electron resonance line has been used to provide the reference signal. The latter spectrum is a simple, isotropic one-line resonance so that one need not be concerned with aligning the sample along a specific direction in these measurements. The transition for the conduction electron occurs between + 1/2 and - 1/2 spin states as it does for the K-center, thus eliminating corrections in transition probabilities between the two resonances. Both the linewidths and intensities of the two resonances are comparable, obviating in most instances changing gains and field modulation amplitudes in going from one spectra to the other. One of the more important features of the conduction electron resonance is that it is well separated in magnetic field from the K-center resonance allowing both to be viewed at the same time. An additional advantage is obtained since in this case the filling factor of the cavity requires no correction.

The actual spin density of the conduction electron sample was calibrated in two ways. One method employed the measurement of the Hall constant and resistivity. Here a silicon slice adjacent to the sample used in the electron resonance measurements was made into a Hall sample and measured at room temperature and at neon temperatures. Since the material is degenerate, one expects the carrier concentration to be the same at both temperatures. This is the case since the results yielded a free carrier concentration of $2.6 \times 10^{18}/cm^3$ and a resistivity, $\rho = 0.042$ Ω-cm, and $2.6 \times 10^{18}/cm^3$ and $\rho = 0.027$ Ω-cm at 27°K and 300°K, respectively. Here, of course, it is assumed that the free carrier concentration is equal to the spin density.

The other way in which the standard sample was calibrated was by spin resonance. The resonance signal of the standard is compared to the resonance signal of a known concentration of phosphorus donors ($3 \times 10^{16}/cm^3$); see Fig. 3. The linewidths of both are known and the areas measured. Taking into account the skin depth of the microwave magnetic field we obtain to within 15% the same spin density as that calculated from the Hall measurements.

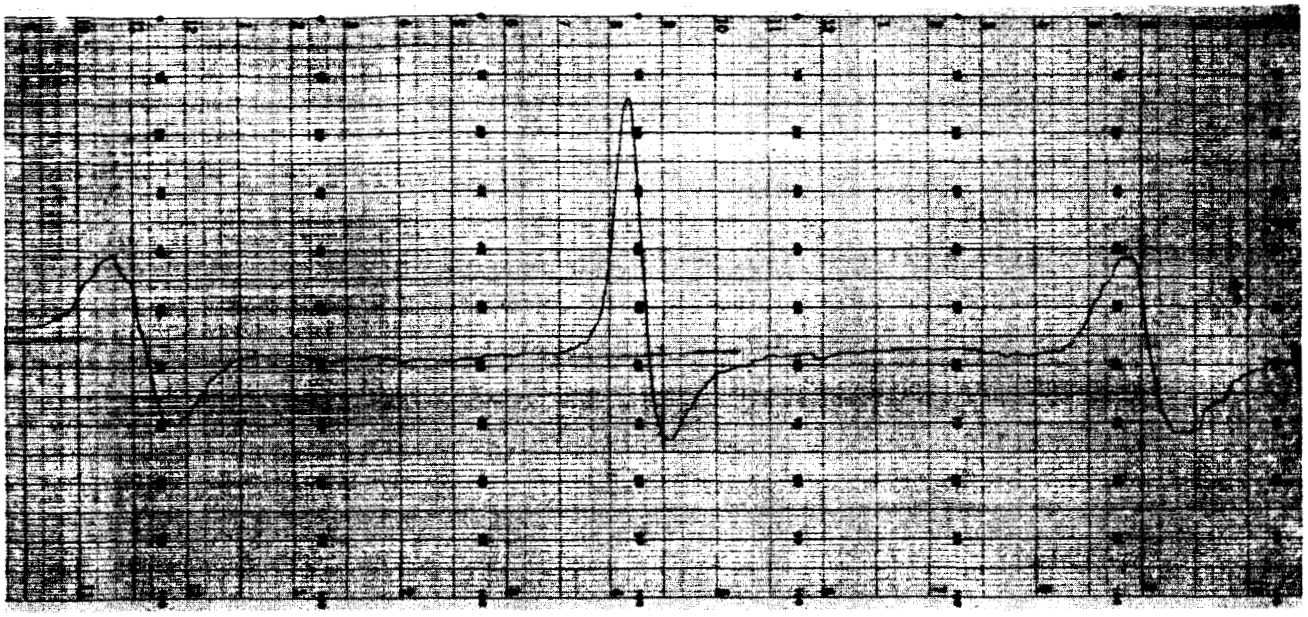

Fig. 3. Comparison of conduction electron resonance with phosphorus doublet lines at the same gains. Total number of spins of phosphorus-doped sample = 1×10^{14}.

The skin depth factor used in the spin density calibration of the standard sample comes about because of the fairly low resistivity of the sample (0.042 Ω-cm). As a result of the low resistivity, the penetration of the r-f magnetic field is confined to a small depth of the sample, δ, which is given by

$$\delta = \left(\frac{\lambda \rho}{120 \pi^2 \mu} \right)^{1/2} \text{ cm}$$

For our sample

$\rho = 0.042$ Ω-cm

$\mu = 1$

$\lambda = 1.4 \text{ cm}^{-1}$

from which we obtain $\delta = 2.2$ mils. Since the magnetic field penetrates both sides of the standard sample the overall skin depth is 4.4 mils. The actual thickness of the sample is 13.5 mils. Thus, in the final calculations a factor of 4.4/13.5 must be applied to the K-center density since only that amount of the conduction electron spins is being measured.

E. EXPERIMENTAL PROCEDURES AND RESULTS

1. Experimental Procedure

All the samples studied were p-type, doped with boron or gallium to a resistivity of 2 Ω-cm. Both "pulled" and float-zone silicon crystals were used in these experiments. The samples were 0.025 in. thick by 0.3 × 0.1 in. and irradiated on one side only since the range of the electrons is much larger than the sample thickness. The 1-MeV irradiations were performed on the Van de Graaff accelerator at RCA Laboratories at a beam current of 5 $\mu A/cm^2$, and the 6.6 MeV run was made with Ethicon's high-voltage linear accelerator. The beam current was maintained at 10 $\mu A/cm^2$. A Faraday cup was used to monitor the current and total charge throughout the irradiations. The samples were kept cool by mounting them on water-cooled blocks. The temperature was recorded during the bombardment with a thermocouple. A 25°C rise was obtained for the lower energy bombardment and 50°C for the 6.6-MeV irradiation.

The spin resonance measurements were performed at liquid neon temperatures with a spectrometer operating at a frequency of 21.5 Gc/sec. The arrangement of the microwave bridge is shown in Fig. 1. In the measurements used for the K-center density calculations, a reference sample (described in Section I-D) containing 8.5×10^{13} spins was placed in the cavity along with the irradiated silicon bars. The spin resonance data were taken only in the dispersion mode at a modulation frequency of 80 cps and a modulation field of 0.32 G.

2. Results

The dominant electron spin resonance spectrum (K-center spectrum) obtained in electron-irradiated p-type silicon consists of seven closely spaced lines. The spectrum is shown in Fig. 4

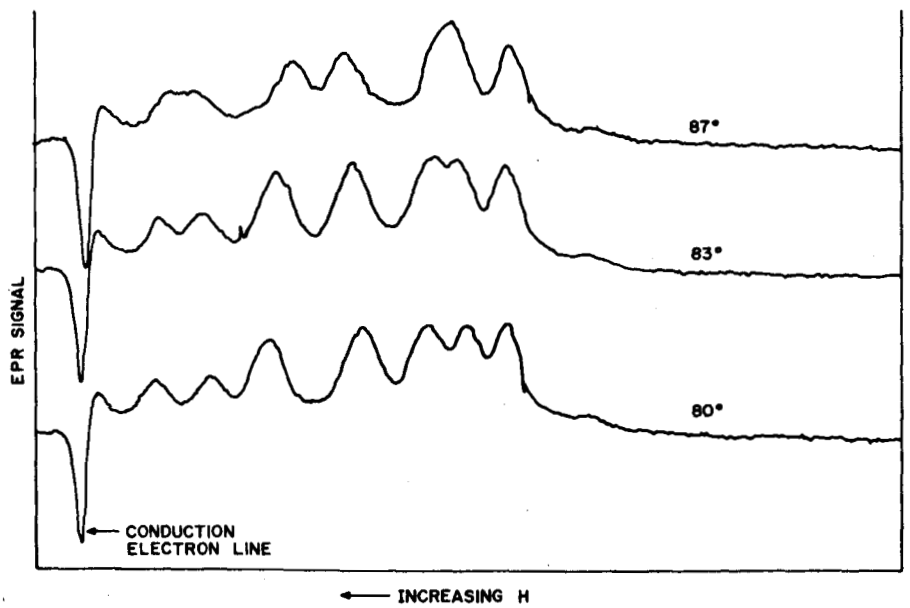

Fig. 4. The K-center resonance spectrum taken with the magnetic field rotated 80°, 83° and 87° from the <100> direction, in the (110) plane.

where the line on the extreme left is that of the silicon conduction electron resonance. The K-center linewidth is about 2.5 gauss as compared with a width of one gauss for the conduction electron line.

The angular variation of the seven-line spectrum has been fully investigated and the details have been discussed in an earlier report. For completeness, however, we will include the pertinent results here. The analysis of the data on the angular variation of the spectral lines with magnetic field (see Fig. 5) is well fitted by a defect whose three principal magnetic axes are along the <221>, <1$\bar{1}$0>, and <11$\bar{4}$> directions. The corresponding g-values are 2.0000, 2.0066, and 2.0056. The direction of the <221> axis is in the line from a lattice site to a next nearest interstitial position.

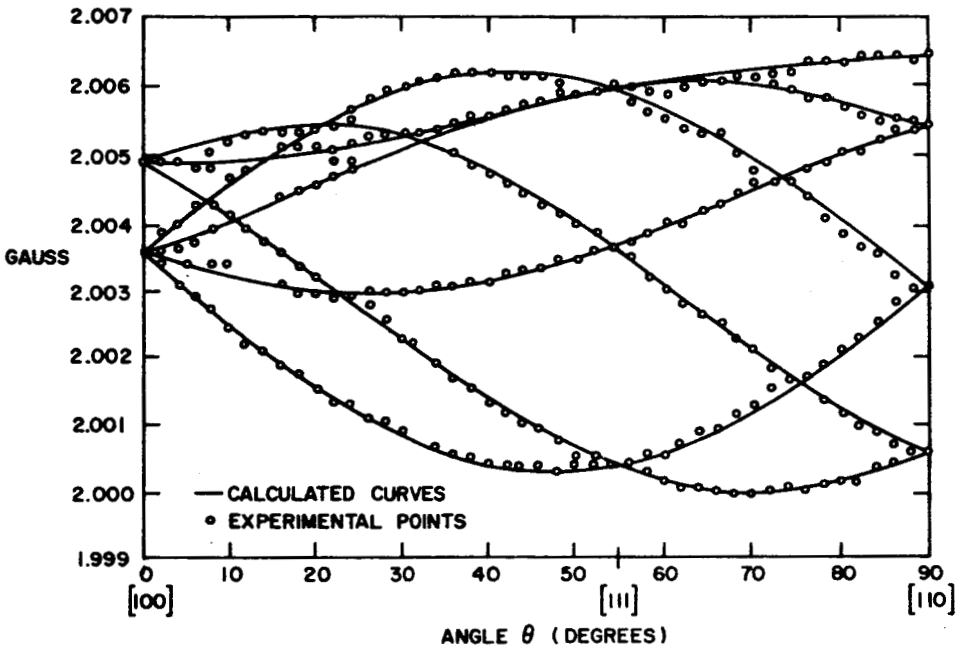

Fig. 5. Angular variation of the K-center resonance lines with magnetic field. H is confined to rotate in the (110) plane.

The K-center spectrum has been detected in both gallium- and boron-doped pulled silicon crystals. The resonance has not been observed in silicon with similar dopings grown by the float-zone technique. The oxygen concentrations in these latter crystals is approximately $10^{16}/cm^3$ as compared with $10^{18}/cm^3$ for the pulled silicon crystals. In the float-zone silicon irradiated at 1 MeV at a flux of 5×10^{16} el/cm^2 only the J-center appears.[4] Part of the J-center spectrum is observed in the pulled crystals along the K-center (see Fig. 6) but because of its low production rate is usually not seen.

Another condition for the detection of the K-center appears to be the resistivity of the material. At large fluxes the density of the damage center decreases and, in some instances, is

not detectable at all. The silicon, in these cases, has undergone a change in the room-temperature resistivity from 2 Ω-cm to 1000 Ω-cm because of the bombardment. After annealing these samples the resistivity is reduced to 35 Ω-cm, and the K-center resonance reappears.

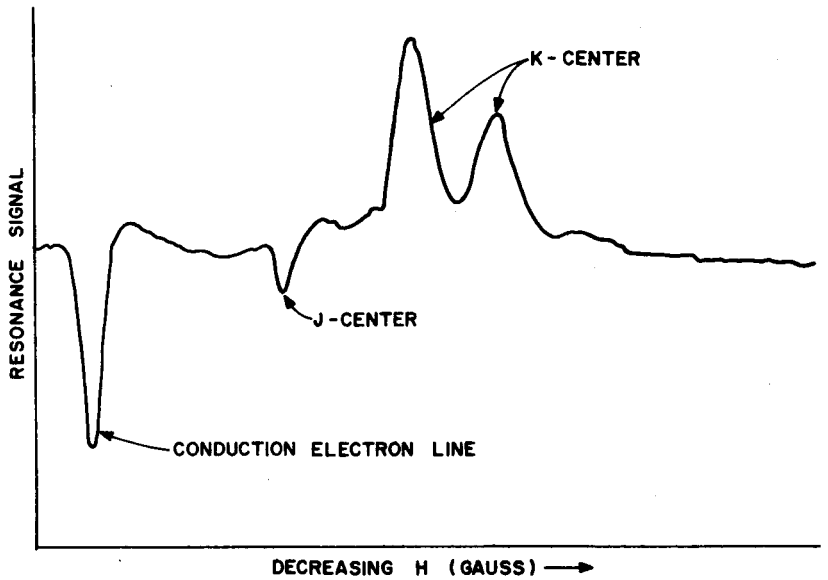

Fig. 6. EPR spectrum of irradiated silicon showing the K-center resonance and part of the J-center resonance [H is perpendicular to the (100) plane.].

The density of K-centers was obtained for irradiations performed at 1 MeV and 6.6 MeV for flux ranges from 10^{16} el/cm^2 to 5×10^{17} el/cm^2. The plot of these data is shown in Fig. 7.

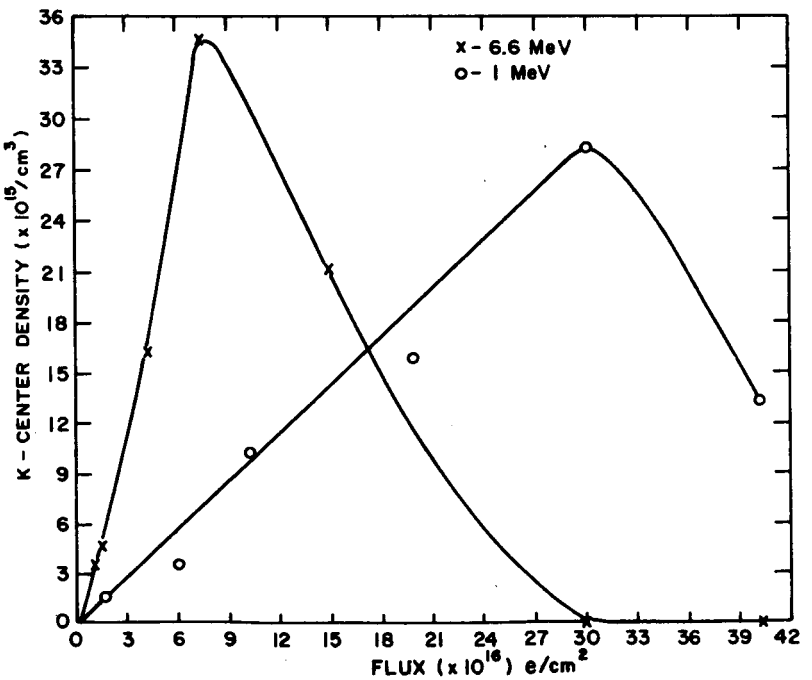

Fig. 7. The dependence of the K-center density on electron flux at 1 MeV and 6.6 MeV.

Two distinct regions are evident in both curves. The division of these two regions occurs at different flux points for the two curves. In the low flux range the defect density is seen to increase linearly with flux. The introduction rates obtained from this part of the curves are 0.1 cm^{-1} and 0.5 cm^{-1} for 1 MeV and 6.6 MeV, respectively. However, these values should be modified to 0.03 cm^{-1} and 0.15 cm^{-1}, respectively, as discussed on page 14. At the higher fluxes the spin density begins to decrease. In fact, for the higher energy irradiation the density diminishes to the point where it is no longer detectable.

Attempts to detect the K-center in silicon irradiated at 700 keV up to fluxes of 5×10^{16} el/cm^2 were unsuccessful. This result indicates that the production rate of this defect falls off sharply between 1 MeV and 700 keV.

The difficulties of making absolute K-center density determinations from electron spin resonance data were pointed out in Section I-D. For this reason, the resonance was investigated as a function of modulation frequency, and amplitude and sweep rate. It was found that both changes in modulation frequency (from 40 cycles to 400 cycles) and the sweep rate of the magnetic field have little effect on the intensity of the signal. This was determined by comparing the resonances of several samples to the signal from the reference sample. Changes in modulation amplitude did, however, change the ratio of the K-center resonance signal to the reference signal. This is to be expected since the linewidths are different. A plot of the amplitude of the K-center and reference signals as a function of modulation field is shown in Fig. 8. The reference signal

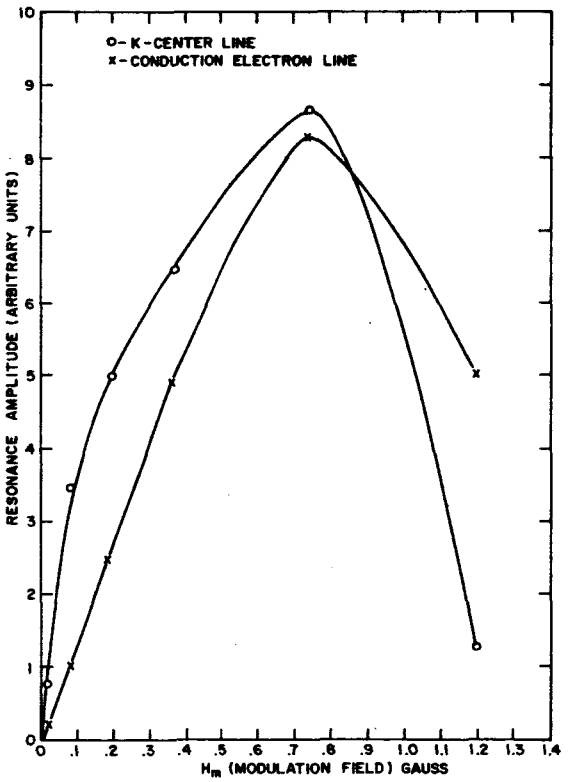

Fig. 8. The dependence of the dispersion resonance amplitude on modulation field.

increases linearly as one might anticipate for a nonsaturated line and then begins to decrease when the modulation field approaches its linewidth. The K-center, on the other hand, behaves according to Weger's[7] prediction for inhomogeneously broadened lines; compare this curve to the bottom curve in Fig. 2. If it is now assumed that the maximum signal obtained represents the total susceptibility (or total spins) of the systems, we can make a determination of the K-center density. We already know the number of spins of the reference sample (see Section I-D). Although in practice a modulation field of 0.32 G was used because it was more convenient in terms of the amplitudes and the shapes of the signals, a simple correction can be made to the spin numbers of the K-center and reference sample from the data presented in Fig. 8.

F. DISCUSSION

The K-center spin resonance data show that it is readily produced in pulled p-type silicon crystals and not in float-zone material. The larger oxygen concentration in the pulled crystals indicates that oxygen is required in the formation of this paramagnetic damage center. Furthermore, the observation of the K-center resonance in silicon containing either boron or gallium demonstrates that the defect is not directly associated with a specific impurity. The presence of the acceptor appears to be necessary in order to provide the proper charge state for detecting the damage center. The evidence for this comes from the combined experimental observations of the failure to detect the center in samples irradiated with large fluxes and the simultaneous change in resistivity of the sample. This is supported by the annealing experiments of these particular samples in which a reduction in resistivity and the re-appearance of the K-center signal are simultaneously brought about. This suggests that the detection of the K-center is dependent upon the location of the Fermi level. Consistent with this picture are the quantitative data of the spin density variation with flux. From Fig. 7 it is seen that the damage density increases linearly with flux up to a certain point. It begins to decrease at a flux of 3×10^{17} el/cm^2 and 7.5×10^{16} el/cm^2 for the 1-MeV and 6.6-MeV irradiations, respectively. The significance of this will become apparent in the next paragraph.

The carrier removal rate in p-type silicon has been investigated thoroughly.[10,11] In Fig. 9 we reproduce Space Technology Laboratories data on the introduction rate of the carrier removal site as a function of energy. It can be seen that this site, which is located at 0.3 eV above the valence band, has an introduction rate of 0.04 cm^{-1} at 1 MeV and 0.2 cm^{-1} at 6.6 MeV, or a ratio of 5:1 in introduction rate. Note also that the initial slopes in Fig. 7 are in the ratio of about 5:1, and since these slopes are proportional to introduction rate, this is good agreement. Using the introduction rates for the carrier removal site we can determine the flux required to change the resistivity of the silicon samples used in our experiments. The original resistivity is between 1 and 2 Ω-cm, representing an acceptor concentration close to 10^{16}/cm^3.

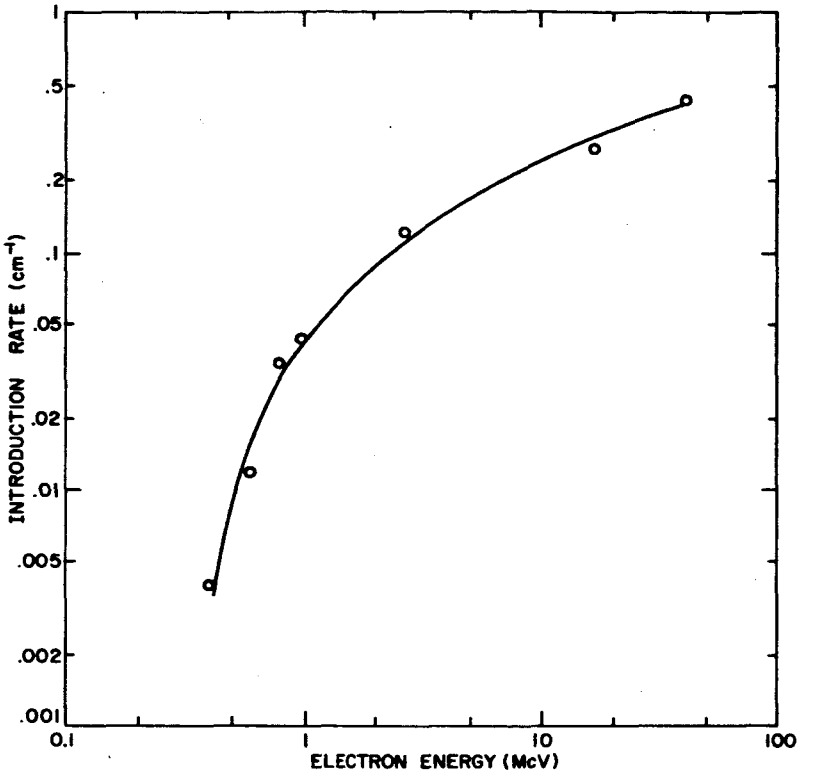

Fig. 9. Electron energy dependence of the $E_t - E_v = 0.3$ eV defect level in p-type silicon according to STL.

We find that the resistivity should change at fluxes of 2.5×10^{17} el/cm^2 and 5×10^{16} el/cm^2 for 1 MeV and 6.6 MeV, respectively. As pointed out above, the production rate of the K-center begins decreasing at 3×10^{17} el/cm^2 and 7.5×10^{16} el/cm^2, suggesting that the carrier removal site at 0.3 eV is responsible for both the change in resistivity of the irradiated silicon and the change in charge state of the K-center. These results can be explained by considering, for the condition of low fluxes, that some of the holes are trapped at the K-center defects. As the K-center density increases, the number of holes trapped also increases. At large fluxes, however, the number of carrier removal sites has increased sufficiently to alter the resistivity and presumably raise the Fermi level through the K-center level. As a consequence, the holes are emptied from the K-center and trapped at the 0.3-eV level. At still larger fluxes, most of the K-centers are empty, resulting in a failure to detect its resonance. This model locates the K-center as lying between the 0.3-eV level and the valence band edge. In view of this, it is interesting to note that Vavilov[12] has reported levels at 0.12 eV and 0.21 eV above the band edge from photoconductivity measurements.

As mentioned above, the charge state of the K-center must be positive since it is trapping a hole. The observed g-values, which show a positive shift from a free electron g-value, are consistent with the association of a positive charge with the K-center.

There is one factor which is not consistent with the above model. This concerns the maximum K-center density calculated from the data. The acceptor concentration is smaller than the K-center density by a factor of 3 to 4. This difference may arise from the assumptions made in trying to assess the K-center density relative to the conduction electron density. As mentioned in Section I-C, it is extremely difficult to take into account all the experimental parameters and permutations of these parameters, germane to the intensity of inhomogeneously broadened resonances, such as the K-center resonance. To actually accomplish this, a thorough theoretical analysis of the K-center resonance shape and amplitude must be made for a number of experimental conditions which has to be verified by actual experiments. The end result of such a study may then yield the absolute density of the damage center. It is felt, however, that the return obtained from such an effort is not justified at this time.

It should be pointed out that the factor of 3 to 4 does not alter the shapes of the curves obtained for the K-center density as a function of flux nor the relative values of the curves on Fig. 7. The points in Fig. 7 are good to within 20% on an arbitrary scale. If we now consider the model presented above as being valid, then the maximum K-center density must be $10^{16}/cm^3$. This in turn would lower the introduction rates to 0.03 cm^{-1} and 0.15 cm^{-1} for the 1-MeV and 6.6-MeV bombardments.

Finally, in regard to the nature of the defect there are two pertinent facts. One has been mentioned earlier and refers to the required presence of oxygen in the production of the K-center. The second fact involves the symmetry axis <221>; i.e., the g-tensor is axially symmetric about the <221> axis. This direction points from a silicon lattice site to the next nearest interstitial position. The simplest picture of the defect, namely a lattice vacancy with an interstitial once removed from it, is inconsistent with Watkins' conclusions[4] that free vacancies are produced by low energy bombardment and these are mobile at room temperature. It is suggested that the center involves a substitution oxygen atom associated with an interstitial silicon atom. Failure to detect any hyperfine interaction, however, has prevented us from exploring further this suggested configuration.

G. CONCLUSIONS AND RECOMMENDATIONS FOR FUTURE WORK

In summary, the spin resonance investigations on irradiated p-type silicon have shown that the dominant paramagnetic defect has principal axes along the <221>, <1$\bar{1}$0>, and <11$\bar{4}$>. The introduction rate of this defect is 0.03 cm^{-1} and 0.15 cm^{-1} at 1 MeV and 6.6 MeV, respectively. The defect level is established as lying between 0.3 eV and the valence band from the variation of defect density with flux. It is suggested from the symmetry axis (<221>) that the defect involves an oxygen in a substitutional site in association with a next-nearest interstitial silicon atom.

The effort concerning the K-center defect is believed to be almost complete. Two items are outstanding. There are samples on hand which have been irradiated at 3 MeV over a range of fluxes from 5×10^{15} el/cm^2 to 10^{17} el/cm^2. Spin resonance measurements of these samples would give us additional data on the K-center similar to that obtained from the 1-MeV and 6.6-MeV irradiations. Secondly, performing corresponding experiments on 0.1-Ω-cm and 10-Ω-cm material would help to verify the explanation given above for the decrease in K-center density with increased flux. Here the peak of the curve would be expected to shift because of the change in acceptor concentration.

It should be pointed out that this is our first evidence of a correlation between EPR properties and electrical properties in silicon. A more precise understanding of the correlation will come about when we make 1-MeV EPR measurements at several different resistivities. If our model is correct these data should show peaks at differing fluxes correlating with the initial Fermi level.

II. THE EFFECT OF IMPURITIES OF RADIATION DAMAGE IN SILICON

A. INTRODUCTION

It has been shown that vacancies introduced by high-energy electron irradiation of silicon form stable defects with impurities.[2] Watkins et al., for example, found that vacancies associate with oxygen in crucible-grown silicon, or with phosphorus in floating-zone n-type silicon.[2] Less explicit evidence of impurity interactions with structural defects (vacancy-interstitial pairs) can be deduced from solar cell experiments.[13] Measurable differences in otherwise identical cells irradiated under the same experimental conditions may be due to defect formation with random trace impurities in the cells. In general, vacancy impurity combinations can be expected to have electrical properties which depend upon the specific impurity involved. For example, the energy levels associated with these defects may occur at different locations in the forbidden energy gap.[14]

It has long been thought that specific impurities might be found which can markedly reduce radiation damage in silicon solar cells. Although silicon solar cells are currently the most reliable energy sources for satellite applications, they are relatively vulnerable to radiation damage. These cells require high minority-carrier lifetime for efficient operation, and this lifetime is very sensitive to radiation. The reduction of lifetime sensitivity to radiation damage by specific impurity interactions with structural defects is the goal of the work described below.

The following impurities have been selected for immediate study: Al, Au, B, Cu, Fe, Ga, Gd, In, and Li. The impurities were chosen for a variety of reasons. Interstitial interactions with Al and vacancy interactions with Au and Cu have already been reported.[15,16] Li and Cu diffuse rapidly as interstitials in silicon; consequently, vacancy interactions with these impurities are more probable. Fe also diffuses rapidly and has the added advantage of being paramagnetic. Thus, spin resonance studies may supplement lifetime studies when Fe is used. The column III elements – B, Ga, and In were chosen to study the effect of the major dopant. Gd has been reported to increase the radiation resistance of solar cells.[17] In addition to the reasons cited above, mass spectrographic analyses of solar cell material suggested the use of B, Cu, and Fe.

The property selected to study the effect of the above impurities experimentally is the diffusion length. While this parameter is not as fundamental as the carrier lifetime, it is more directly related to the solar cell short-circuit current. Furthermore, a convenient, steady-state method of measuring the diffusion length is available.[18] The following sections discuss the work performed to date.

B. THEORY AND EXPERIMENTAL TECHNIQUES

1. Theory

The specific parameters which will be used in this study arise from the equation relating minority-carrier lifetime τ to the bombardment flux ϕ. If we assume the total rate of minority-carrier recombination is equal to the sum of the rates at various centers, τ is given by[19]

$$\frac{1}{\tau} = \frac{1}{\tau_0} + (\eta\sigma v f)\phi \tag{2}$$

where τ_0 is the initial lifetime, η is the introduction rate of recombination centers in No./cm, σ is the recombination cross section in cm^2, v is the thermal velocity of the minority carrier, f is the fraction of centers which contain a majority carrier (the filling factor), and ϕ is the incident flux in No./cm^2. Since the diffusion length is related to τ and the minority carrier diffusion constant D as

$$L^2 = D\tau, \tag{3}$$

Eq. (2) can be rewritten in terms of L as

$$\frac{1}{L^2} = \frac{1}{L_0^2} + \left(\frac{\eta\sigma v f}{D}\right)\phi = \frac{1}{L_0^2} + K\phi. \tag{4}$$

The parameter K (not necessarily a constant!) contains the properties associated with a recombination center together with the Fermi level and temperature dependence through the filling factor f. Therefore, K was chosen to study impurity interactions in irradiated silicon. Of course, careful account of the resistivity and temperature must be made in evaluating experimental data because of the presence of the filling factor in K.

The value of K can be determined by fitting Eq. (4) to the experimental data with the measured value of L_0. Alternatively, since

$$L = (K\phi)^{-1/2} \tag{5}$$

at high fluxes, any point in the high-flux region can be used to find K. The experimental data on a log-log graph should have a slope of 0.5 according to Eq. (5).

The other parameter chosen for this study is the diffusion length L_f after a specified flux. The flux used here has arbitrarily been set as 2×10^{15} el/cm^2 at which value Eq. (5) is generally applicable. The value of L_f is a convenient number which is related more directly to solar cell performance.

2. Measurement of the Diffusion Length L

The response m of a solar cell to penetrating radiation is defined as

$$m = I_{sc}/I_B = S(L_s + L_B), \tag{6}$$

where I_{sc} is the short-circuit current in amperes, I_B is the incident current of the penetrating radiation in amperes, S is the specific ionization produced by the radiation (corrected for reflection from the cell surface) in pairs/cm, and L_s and L_B are the diffusion lengths on both sides of the junction in cm. If S is known, the sum of the diffusion lengths can be determined from a measurement of I_{sc} and I_B.

Although Eq. (6) is written in terms of $L_s + L_B$, the diffusion length L_B in the base region of a silicon solar cell far exceeds the diffusion length L_s in the diffused or "skin" region even after a substantial irradiation. For example, L_s is typically less than the junction depth which is on the order of 0.5 μ while L_B exceeds 100 μ before and 10 μ after irradiation with 5×10^{15} el/cm^2 (1 MeV). Consequently, Eq. (6) can be rewritten solely in terms of L_B with very little error. Because of this argument, the distinction between L_B and $(L_s + L_B)$ is not preserved below; the experimental value of L is to be taken as indicative of the base material of the solar cell.

A convenient technique[18] is available for determining L. The penetrating radiation used is a beam of 1-MeV electrons with a sufficiently low intensity and duration so as not to change significantly the parameter being measured. The range[20] of 1-MeV electrons in silicon is 66.5 mils; hence, these particles easily penetrate the 10-mil (or less) active region of a silicon solar cell. Almost all of their energy is lost in producing ionization in the crystal. Because of the energy loss, the ionization varies with depth, reaching a maximum value at a certain depth.[21] While the specific ionization can be computed in principle,[21] it is sufficiently difficult to warrant an experimental measurement, especially since the experimental arrangement will influence the value obtained. An ionization curve is measured by placing absorbers, preferably of silicon, but actually (more practically) of Al which has almost the same density, before a cell which is sufficiently damaged so that L does not change, and measuring the resulting I_{sc} for a given I_B. In effect, the absorbers move the junction to various depths where the ionization produced by the beam is sampled. Since most of the beam energy is used in producing electron hole pairs with an average expenditure of 3.6 eV/pair in silicon,[22]

$$\int_0^\infty S\,dt = \frac{1}{L} \int_0^\infty \frac{I_{sc}}{I_B}\,dt = \frac{\rho E}{3.6} \tag{7}$$

where t is the absorber thickness in g/cm^2, E is the incident electron energy, and ρ is the density of silicon (2.328 g/cm^3). The value of L is determined from the area under the curve of I_{sc}/I_B vs. t and the other known quantities. Once L is known, S can be specified since

$$S = \frac{1}{L} \frac{I_{sc}}{I_B} \tag{8}$$

Besides obtaining S from these measurements, one also obtains the absorber thickness for which the maximum specific ionization S_0 occurs. Subsequent measurements of L in solar cells are made using this absorber thickness. The use of the maximum value of S is preferred, of course, since the variation of S with thickness at this value is a minimum.

Two corrections should be made to the value of S_0. First, some of the electron energy is backscattered from the absorber surface.[23] The value of S_0 is multiplied by 0.964 to account for this effect.[23] Secondly, the energy loss for the incident electrons depends not only on the absorber thickness but also on the number of electrons per gram of absorber; i.e., on Z/A where Z is the atomic number and A is the atomic mass.[20] In the experimental arrangement, aluminum is used to reduce the particle energy while silicon is used to measure the rate of energy loss. Since

$$(Z/A)_{Al} = 0.96\ (Z/A)_{Si}, \tag{9}$$

thicker aluminum than silicon absorbers are required to produce the same particle energy. Consequently, the area under the ionization curve is overestimated by 1/0.96. To accommodate this correction, S_0 should be multiplied by 1/0.96. The total correction to the value of S_0 is $0.964/0.96 \approx 1$.

3. Device Structures

The method chosen for measuring L requires a junction to separate the electron-hole pairs produced by the ionizing beam. Two requirements were imposed on the method of preparing the junction to insure that we study impurity effects and not merely techniques of junction fabrication. First, the junction must be formed easily, so that a minimum of time is spent on device fabrication. Secondly, all processing temperatures should be as low as possible to prevent effects due to heat treatment from obscuring impurity effects. To achieve these aims, we first studied surface barrier devices using a suitable metal deposited on a suitably prepared blank of p- or n-type conductivity.[24,25] Because it was difficult to duplicate the diffusion length values found in solar cells when the surface barrier structure was used on p-type material, we adopted another process involving lithium, one of the impurities under study in this program. Lithium is a donor which diffuses rapidly in silicon, so that it can be used to form a junction at a low temperature. This diffused structure was used for p-type, while the surface barrier was used for n-type silicon.

C. RESULTS

1. Specific Ionization

The specific ionization has been measured in a number of solar cells made by standard phosphorus diffusion or by lithium diffusion using an experimental setup which has been adhered to since the start of this program. In this setup, the cells are mounted in air on a copper disc 1-1/2 inches away from the beam output window of the Van de Graaff generator. The output window is 1.5-mil aluminum. The thickness of this window and the aluminum equivalent for the air space (1.8 mils) was added to the absorber thickness used in computing S_0. The actual absorber was located within 1/2 inch of the cell face. Since the beam was scanned horizontally and vertically to cover an area of at least 4 cm^2 while the cell area was generally less than 1 cm^2, no correction for multiple scattering was required to account for the cell-absorber separation.[26]

The nominal beam energy was 1 MeV. Aluminum absorber measurements coupled with a Katz and Penfold analysis[27] indicated that the true beam energy was closer to 1.1 MeV. The value used in the calculation of S_0 was 1 MeV.

Typical results obtained are shown in Fig. 10 where m is plotted vs. Al absorber thickness for a phosphorus-diffused solar cell. Four runs taken over an extended time interval are shown

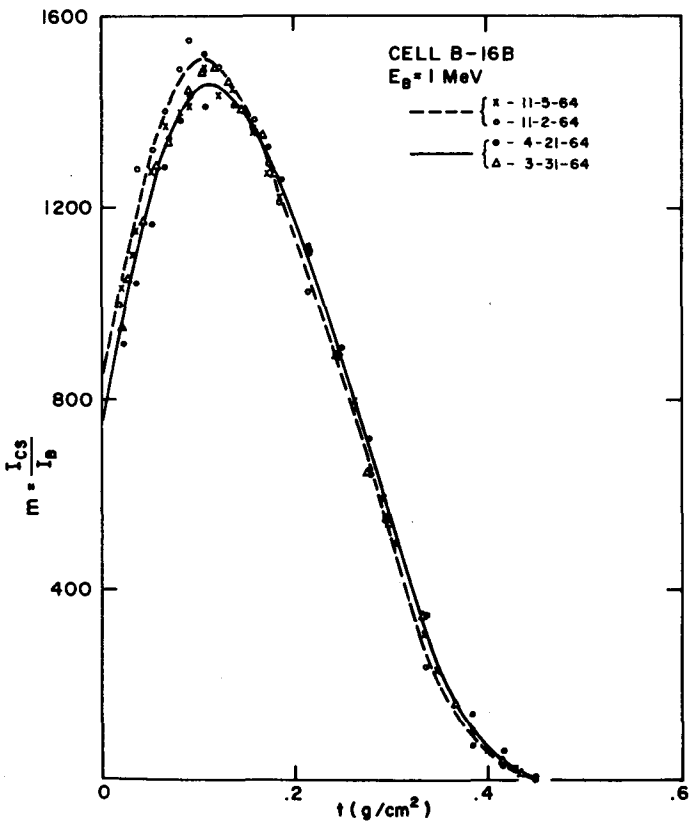

Fig. 10. m vs. aluminum absorber thickness.

to illustrate the reproducibility of this measurement. Small changes are seen to occur which probably arise in slight variations in absorber position, beam distribution, etc. A measure of these changes is obtained from a comparison of the value of S_0 for 12 mils of aluminum, the aluminum absorber thickness for the peak value of S, the value of L from an integration of the curve area, and the value of L obtained by dividing the value of m at 12 mils of aluminum by 254 (see below). This comparison is shown in Table I. A 3% back-scatter correction was incorporated in these values. The net correction as seen above is unity; however, the back-scatter correction has been used throughout this study to maintain consistency with early work.

TABLE I

PARAMETERS FROM FIG. 10.

CURVE	S_0 (PAIRS/μ)	t (MILS)	L(μ)	
			FROM CURVE AREA	m/254
3/31/64	252	13.5	5.9	5.8
4/21/64	244	14.2	5.9	5.6
11/2/64	262	12.4	5.8	6.0
11/5/64	251	13.5	5.9	5.7

The largest variation in Table I occurs in the absorber thickness for the peak value of S; otherwise, the variations are approximately ± 4% of the average value. These results have been covered in some detail to illustrate and emphasize the long time reproducibility, as well as the accuracy, of the subsequent data.

Early measurements of S_0 with 12 mils of aluminum absorber yielded a value of 254 pairs/μ with a 3% back-scatter correction. Subsequent measurements on a total of 25 (phosphorus- and lithium-diffused) cells indicated an average value of 257 pairs/μ with a standard deviation σ_d of 6. The average absorber thickness for peak ionization was 11.8 mils with a σ_d of 1.3 mils. The published value of S_0 for 12 mils of aluminum is 225 pairs/μ for a beam energy of 1 MeV.[18] If our value of 257 pairs/μ is corrected for the higher beam energy of 1.1 MeV, it becomes 234 pairs/μ, 4% higher than the published value.

An S_0 value of 254 pairs/μ with 12 mils of aluminum was used throughout this study. The experimental fixture was used for irradiating the cells as well as for the diffusion length measurements. Initial and periodic measurements of L were made by reducing the beam intensity by one to two orders of magnitude, inserting the 12-mil absorber by remote control and quickly measuring the short-circuit current of the cells. Beam-current measurements were made with an evacuated

Faraday cup. The data were analyzed to find the slope of L vs. ϕ, the value of K, and the diffusion length remaining after 2×10^{15} el/cm^2. The following sections present the results obtained on n- and p-type silicon doped with various impurities.

2. n-type Silicon

In adhering to the requirements of minimum processing and heat treatment, we used Au surface barriers on carefully prepared n-type blanks. If the surfaces were not well prepared, the resulting structure had a low value of L. Subsequent irradiation of these units led generally to large values of K and to slopes of L vs. ϕ different from 0.5. An arbitrary lower limit of 100 μ for the initial value of L was used as a criterion for selecting cells for subsequent irradiation and analysis. Adoption of this criterion led to results more typical of those obtained with diffused cells.

The material studied was phosphorus-doped, oxygen-free, low dislocation silicon supplied by Texas Instruments, Inc. Material resistivities were 1 and 10 Ω-cm. The impurity investigated was lithium-diffused uniformly throughout the blanks. This material was compared with untreated and heat-treated material which had undergone the same processing and heat treatment as the lithium-diffused material except that lithium was excluded. Since lithium is a donor, its addition resulted in a large drop in resistivity. Consequently, the results must be carefully compared to eliminate effects due merely to a variation of resistivity in the three groups of cells.

An example of the diffusion length data for three samples, one untreated, one heat-treated and one lithium-diffused, are shown in Fig. 11. Heat treatment invariably resulted in an L_0 value

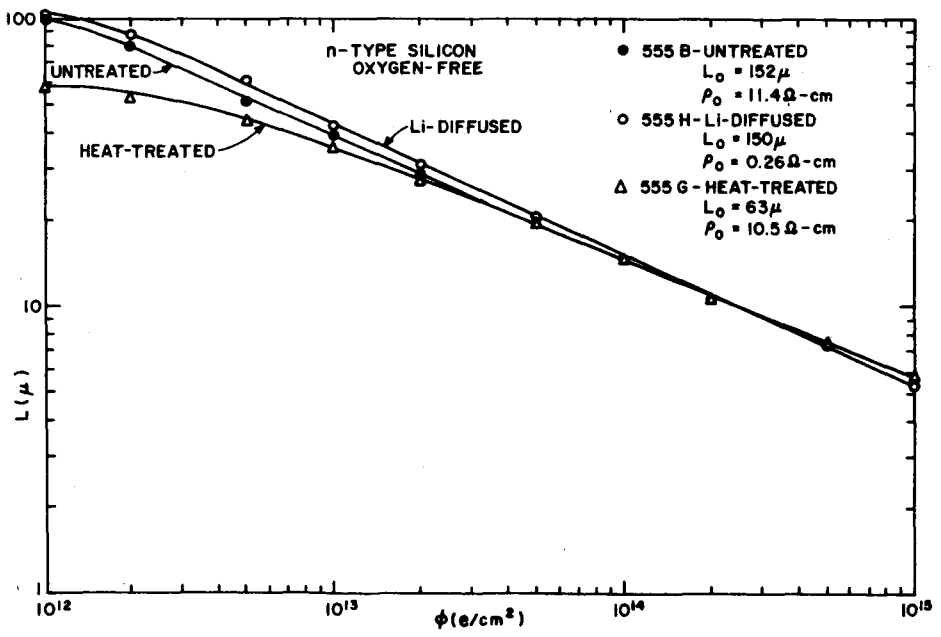

Fig. 11. L vs. ϕ for surface barrier cells.

below 100 μ. When lithium was diffused into the sample, however, L_0 was comparable to the value in untreated material. Figure 11 shows that the value of L_f is comparable for the three types of cells in spite of the variation in L_0. The convergence of the experimental data at high fluxes is surprising since the resistivity of the lithium-diffused sample is 40 times less than the untreated and heat-treated samples.

The same type of behavior was observed in both the 1- and 10-Ω-cm cells. Figure 12 shows L_f vs. the sample resistivity before bombardment. Each point represents one cell. In spite of the addition of lithium with a marked reduction in resistivity, L_f has essentially the same value in the lithium-diffused cells as in the untreated cells. It is as if the material remembered its initial resistivity and behaved accordingly.

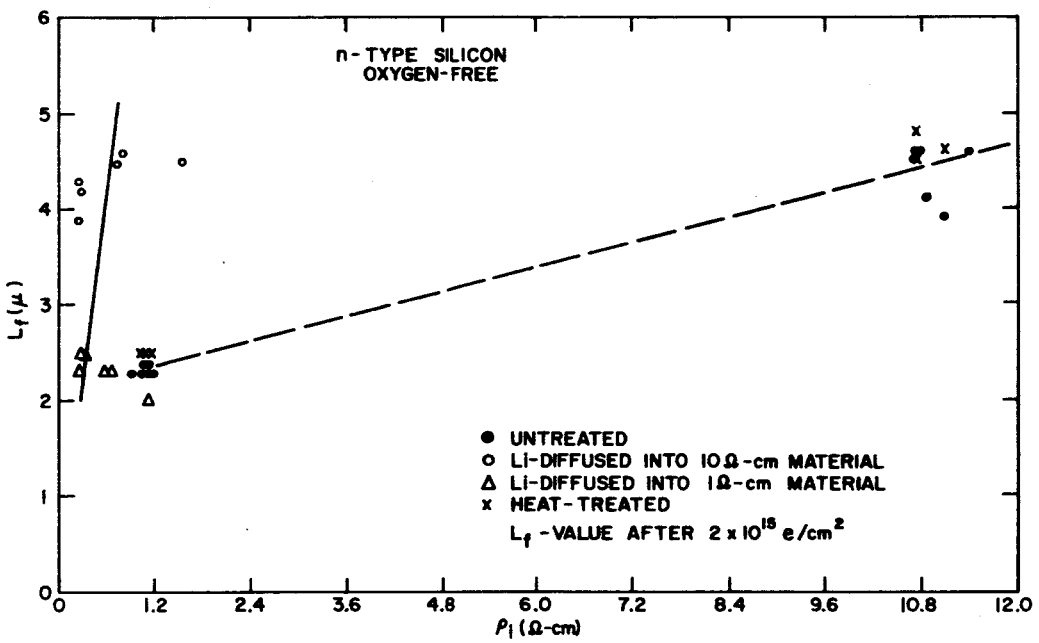

Fig. 12. L_f vs. resistivity for surface barrier cells.

The value of 1/K is plotted vs. sample resistivity before bombardment in Fig. 13. The same value of 1/K is obtained in all cells made from the same starting material, even though the lithium-diffused cells have a much lower resistivity. Some objection may be made here since the slope of L vs. ϕ was not exactly 0.5 for all of the cells. The range of values found for the slope is shown in Table II. Although these values do not agree well with theory, K was computed from Eq. (4) using the initial value of L and its value after a flux of 1×10^{14} el/cm^2. The disagreement between theory and experiment in the value of the slope is discussed on the following pages.

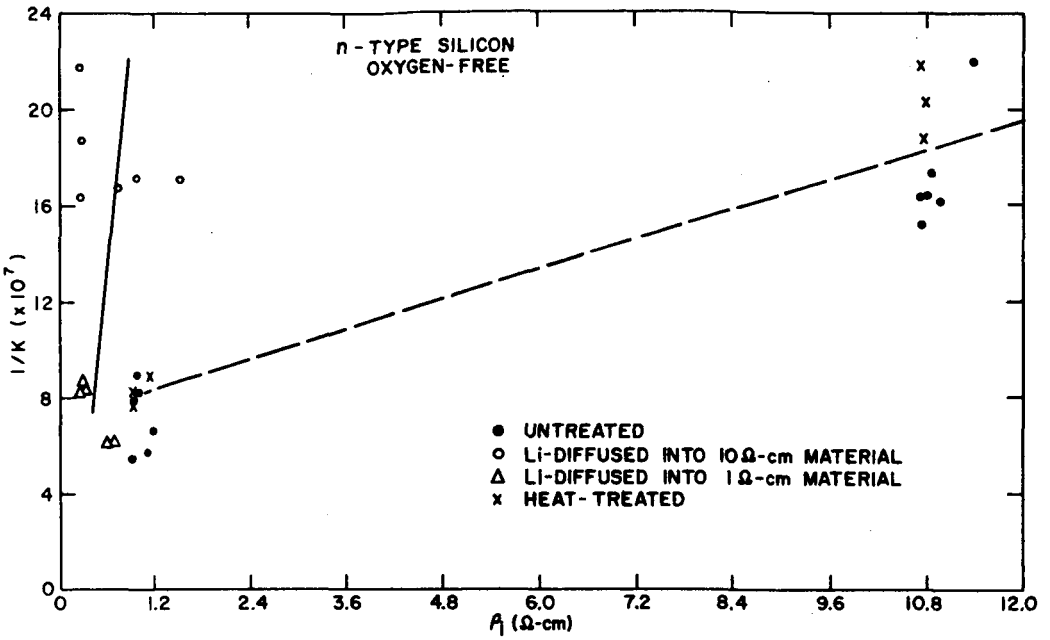

Fig. 13. 1/K vs. resistivity for surface barrier cells.

TABLE II

SLOPE OF L VS. ϕ

CELL	SLOPE
1 Ω-cm untreated	0.45 – 0.48
1 Ω-cm heat-treated	0.41 – 0.47
1 Ω-cm Li-diffused	0.47 – 0.49
10 Ω-cm untreated	0.40 – 0.43
10 Ω-cm heat-treated	0.40 – 0.41
10 Ω-cm Li-diffused	0.44 – 0.45

While the discussion will reconsider the results of this section, some points can appropriately be made here. It can be argued that the above results are only consistent with the degradation of the surface barrier and not of the base material. While this argument cannot be completely refuted at present, the following considerations show the data to be self-consistent. First, the untreated and heat-treated samples have the proper trend with resistivity; i.e., L_f and 1/K are higher for higher base resistivity. Obviously, some knowledge of the base resistivity has been imparted to the results. Secondly, although L_f and K values are not available for B-diffused cells made from the same material, these values can be compared to those obtained on

cells made from other n-type material. A group of Heliotek cells made from 1 Ω-cm, oxygen-containing material had L_f values ranging from 2.9 to 3.1 μ and 1/K values from 1.6 to 1.7×10^8. Values of 1/K reported by STL are $0.49 - 1.8 \times 10^8$ for 1-Ω-cm, oxygen-free cells; $0.72 - 1.1 \times 10^8$ for 1-Ω-cm Heliotek cells; and $2.7 - 6.7 \times 10^8$ for 10-Ω-cm, oxygen-containing cells.[11] These values compare favorably with those found for the surface-barrier cells; namely, an L_f value of 2.0 to 2.5 μ and a 1/K value of 5.6 to 9×10^7 for the 1-Ω-cm cells, and 1.5 to 2.2×10^8 for the 10-Ω-cm cells. The surface-barrier cells gave results then which are reasonable.

3. p-type Silicon

Although the surface barrier gave results typical of n-type material, its use generally led to atypical results for p-type material. In most cases, L_0 was well below 100 μ, and the values of L_f and 1/K were smaller than those obtained with phosphorus-diffused cells. The problem apparently was due to improper surface preparation and to changes occurring in the surface barrier during the irradiation in air. Only in isolated cases were the results consistent with those obtained with phosphorus-diffused cells. Because of this difficulty, the junctions on p-type material were made by diffusion with phosphorus or lithium.

The base impurities which were studied were Al, B, Cu, Fe, Ga, Gd, and In. Experiments in which lithium is incorporated throughout the base region, as opposed to those where lithium is used solely to form the junction, are just beginning and will not be reported here. Of the above impurities, Cu, Fe, and in some cases, Al and Gd, when added to the crystal either during growth or by diffusion, severely reduced L_0 to 50 μ or less, so that meaningful results could not be obtained. (These low values of L_0 occurred in both the phosphorus- and the lithium-diffused cells; however, L_0 was invariably higher in the lithium than in the p-diffused cells.) To study the effect of these impurities, then, smaller amounts must be added to the crystal to preserve the value of L_0.

Typical data obtained in this study are shown in Fig. 14 for phosphorus- and lithium-diffused cells made from similar base material and with the same value of L_0. The figure shows that the lithium-diffused cell is more radiation-resistant than the phosphorus-diffused cell. The slope of the curve for the lithium-diffused cell is 0.39 while that for the phosphorus-diffused cell is 0.50, in spite of the fact that the base resistivity is the same in both cases. The significance of these slopes will be discussed below.

Figures 15 and 16 show the data obtained with the phosphorus-diffused cells. The value of L_f after a flux of 2×10^{15} el/cm^2 is given in Fig. 15 as a function of base resistivity for B, Al, Ga, In, Gd and oxygen-free material. The value of 1/K is shown in Fig. 16 for the same materials. Each point in both figures represents either one or several cells. Considerable scatter is evident in both figures, particularly Fig. 16; so the line has been drawn to represent the trend of the data. The conclusion drawn from these data is that Al, B, Ga, In, and Gd do not increase the

radiation resistance of solar cells in the resistivity range investigated. One-Ω-cm oxygen-free material is significantly poorer than oxygen-containing material; for 10-Ω-cm material, the oxygen-content appears to be immaterial.

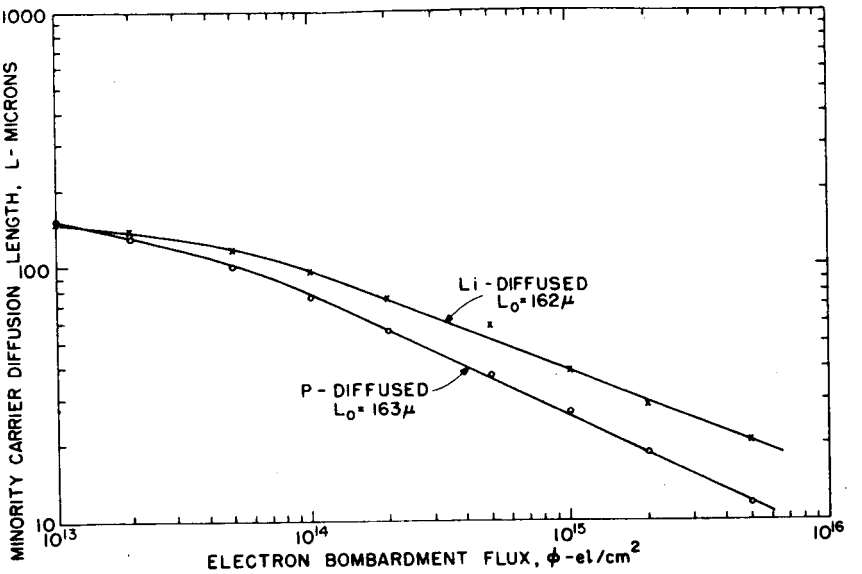

Fig. 14. Comparison of phosphorus- and lithium-diffused cells.

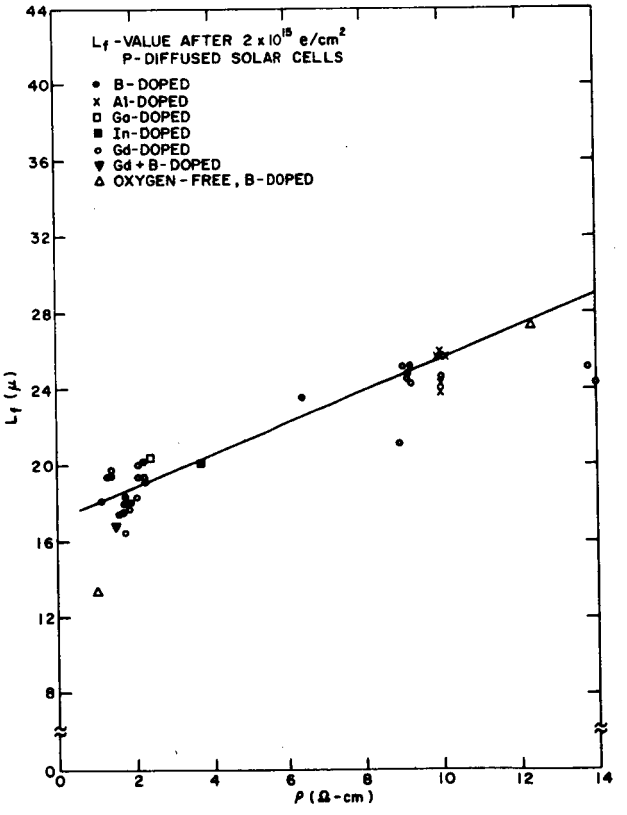

Fig. 15. L_f vs. resistivity.

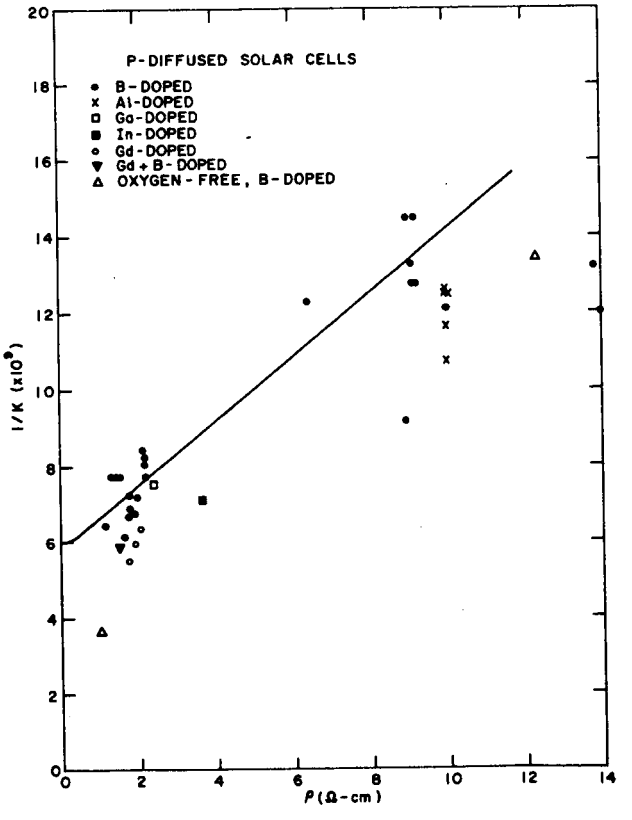

Fig. 16. 1/K vs. resistivity.

The results obtained with lithium-diffused junctions in B- and Al-doped material are shown in Figs. 17 and 18. Each point represents one cell. The lines in both figures represent the range of values which were found with the phosphorus-diffused cells. The data in both Fig. 17 (L_f) and Fig. 18 (1/K) indicate that lithium-diffused junctions are generally more radiation-resistant than phosphorus-diffused junctions for a base resistivity of approximately 2 Ω-cm. Fewer data are available for 10-Ω-cm material; hence, the significance of the data in this region is uncertain.

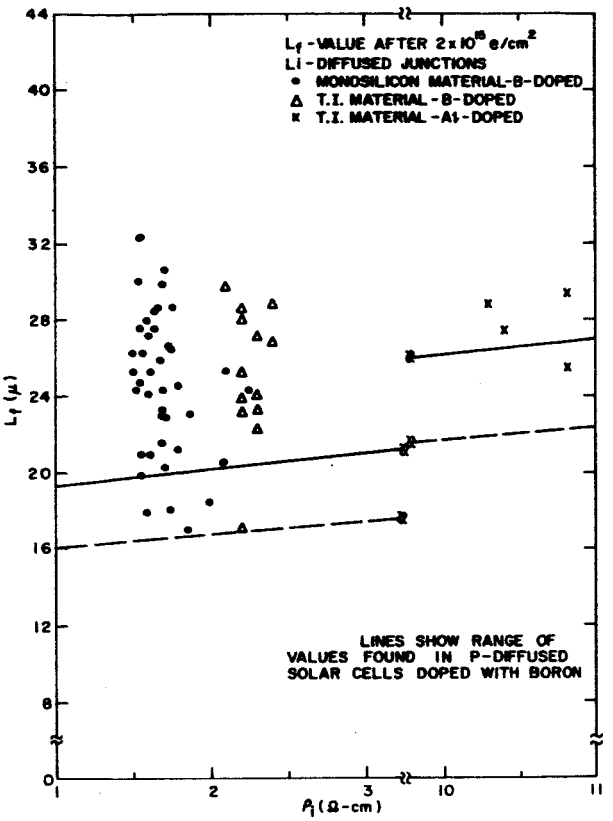

Fig. 17. L_f vs. initial resistivity.

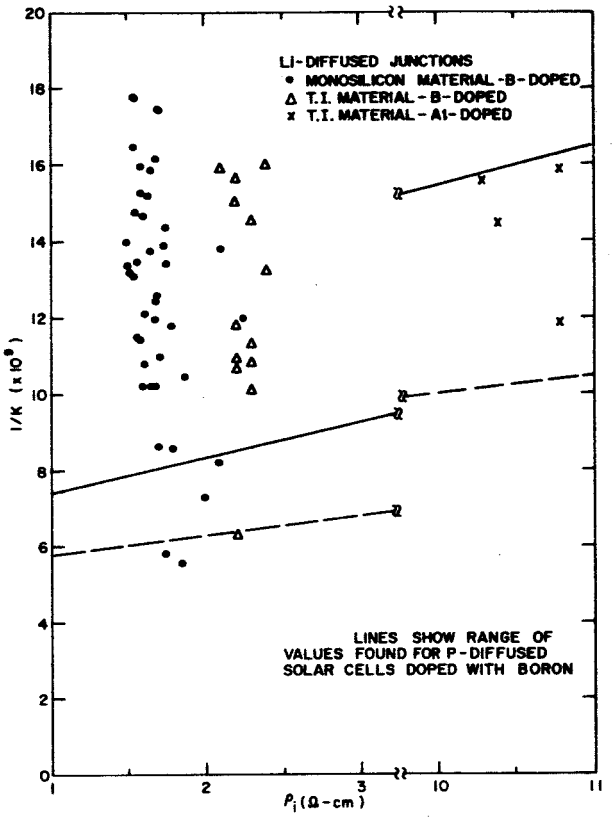

Fig. 18. 1/K vs. initial resistivity.

The data in Figs. 17 and 18 were obtained from cells which were similarly processed. One significant difference between these cells and those made with phosphorus is the junction depth. Because lithium diffuses so rapidly in silicon, it is difficult to fabricate a cell with a junction depth of only 1 μ. The influence of a deep junction on the results was investigated by fabricating a series of junctions and subsequently etching or lapping the diffused surface to reduce the junction depth. The results obtained on one series of cells are shown in Figs. 19 and 20 where L_f and 1/K, respectively, are plotted vs. junction depth. Each point represents one cell. A gradual downward trend is observed in both figures as the junction depth is reduced. The extrapolated values of the lines sketched to represent the data exceed those observed in phosphorus-diffused cells with a junction depth of ~ 0.5 μ. Even though the extrapolated values look promising, however, thinner junction depths are obviously required to demonstrate conclusively the enhanced radiation resistance of lithium-diffused cells.

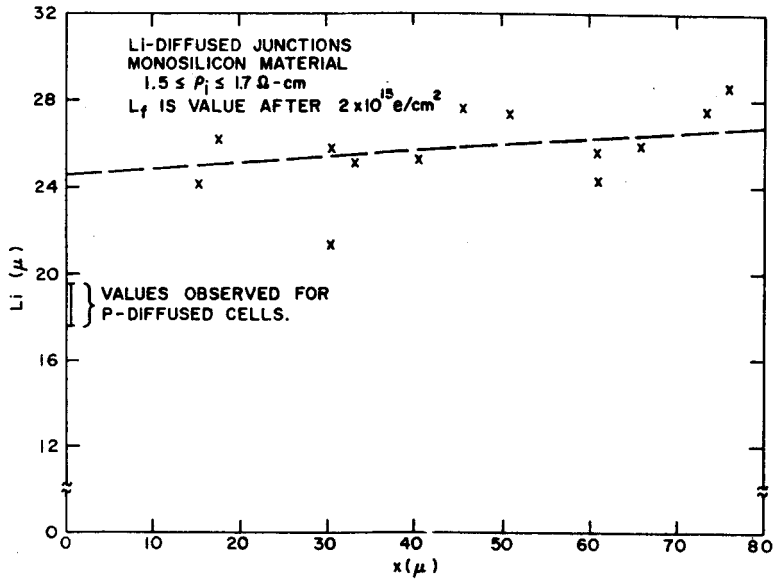

Fig. 19. L_f vs. junction depth.

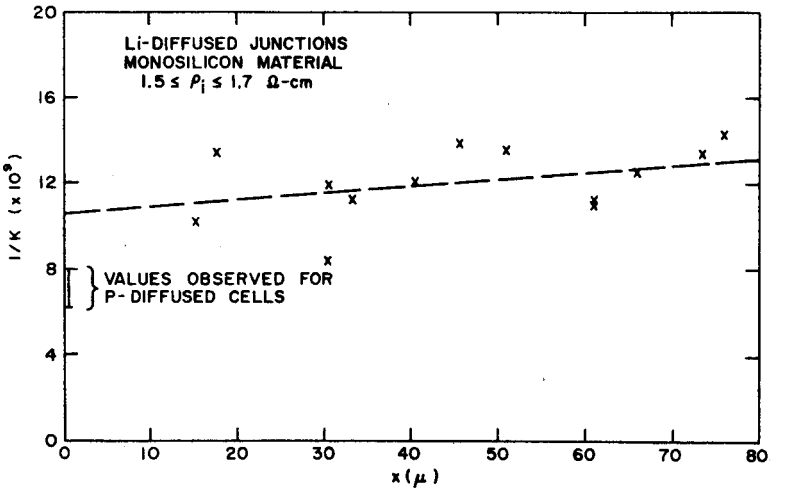

Fig. 20. 1/K vs. junction depth.

Another possible consequence of the rapid diffusion rate of lithium is an increase in base resistivity due to compensation. Attempts to establish the carrier concentration in the vicinity of the junction by capacitance measurements have been unsuccessful at present. The junction is deep and the depletion width penetrates both sides; consequently, analysis of the capacitance data is not straightforward. Four-point-probe measurements on the base material, into which lithium was diffused to form the junction, have not indicated any substantial change in base resistivity as a result of the junction formation. Because this measurement is a volume-average, however, further work with capacitance measurements is obviously required.

Another difference in the lithium- and phosphorus-diffused cells, besides the values of L_f and K, is the slope of the L vs. ϕ data. The range of values observed for the slope is shown in Table III. The theoretical slope of 0.5 is obtained only from low-resistivity phosphorus-diffused cells. The slope decreases for the high-resistivity phosphorus-diffused cells, and much more so for the lithium-diffused cells. In spite of this disagreement with theory, the K values shown above were determined from Eq. (4) using the values of L_0 and L_f after a flux of 1×10^{15} el/cm^2.

TABLE III

SLOPE OF L VS. ϕ

BASE MATERIAL	P-DIFFUSED CELLS	Li-DIFFUSED CELLS
1.5 Ω-cm boron	0.45 – 0.50	0.33 – 0.44
9-10 Ω-cm boron	0.40 – 0.48	–
1 Ω-cm boron, oxygen-free	0.48 – 0.51	0.37
12 Ω-cm boron, oxygen-free	0.45 – 0.46	0.37
10 Ω-cm Al	0.39 – 0.43	0.36 – 0.37
3.7 Ω-cm In	0.42 – 0.44	–
2.4 Ω-cm Ga	0.44 – 0.46	–
2 Ω-cm Gd	0.43 – 0.49	–
1.5 Ω-cm boron and Gd	0.45 – 0.46	–

Some remarks about this slope in the high-resistivity and lithium-diffused cells are appropriate here. The slope will be only 0.5 according to Eq. (5) if K is a constant; that is, independent of flux. Several factors, all of which may occur in practice, can lead to a flux dependence for K. First, Eq. (5) is based on a recombination scheme with only a single energy level in the forbidden gap, whereas a many-level scheme may actually be more appropriate. Secondly, the introduction rate of the recombination centers has been assumed constant when it may very well have a Fermi-level dependence. Finally, the filling factor has been assumed constant while it obviously is not since radiation introduces carrier removal sites, as well as recombination levels, with a consequent movement of the Fermi level. To illustrate how changes in the filling factor alone vary the dependence of L on ϕ, let us examine explicitly the dependence of K on the carrier density p.

$$K = \frac{\eta\sigma v}{D} \frac{\exp (E_r - E_v)/kT}{(N_v/p) + \exp (E_r - E_v)/kT} \tag{10}$$

where $(E_r - E_v)$ is the position of the recombination level with respect to the valence band, N_v is the density of states in the valence band, and the other symbols have their customary or previously

assigned meanings.* The carrier density is a function of flux as follows

$$p \sim p_0 - \eta_c \phi, \tag{11}$$

where p_0 is the initial density and η_c is the carrier removal rate. For 1-MeV electrons in 1-2-Ω-cm material at room temperature, η_c is ~0.2 per cm in n-type silicon and ~0.02 per cm in p-type silicon.[28] The behavior of L in p-type material, based on Eqs. (3), (10), and (11) was computed for several values of η_c and initial base resistivity, and is shown in Fig. 21. The parameter values shown in Table IV were used in the calculations.

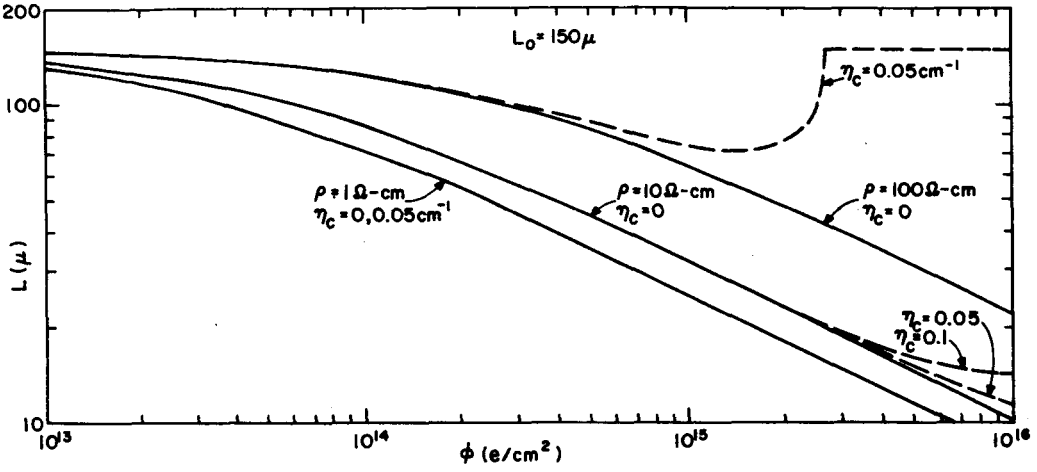

Fig. 21. Computed diffusion length vs. ϕ for various carrier removal rates.

TABLE IV

PARAMETER VALUES USED IN COMPUTING L

PARAMETER	VALUE
σ	1.6×10^{-14} cm^2
v	5×10^6 cm/sec
D	25 cm^2/sec
N_v	1.14×10^{19} cm^{-3}
$(E_r - E_v)$	0.24 eV
L_0	150 μ

*Equation (10) illustrates how the level $(E_r - E_v)$ can be determined experimentally by plotting 1/K vs. 1/p, or ρ if the carrier mobilities are known. For example, using drift mobilities from Cronemeyer, Phys. Rev. **105**, 522 (1957), and conductivity mobilities from Prince, Phys. Rev. **93**, 1204 (1954), and assuming the recombination level is in the lower half of the forbidden gap, $(E_r - E_v)$ will be approximately 0.25 eV in the oxygen-containing and approximately 0.19 eV in the oxygen-free phosphorus-diffused cells irradiated in this program.

Excluding the curve for a base-resistivity of 100 Ω-cm and an η_c of 0.05 cm^{-1}, the shape of which is due to the ineffectiveness of the chosen recombination level when the Fermi-level rises above it, one can determine an apparent slope by fitting a straight line to the high-flux region. The apparent slopes which would be obtained are listed in Table V. A slope lower than 0.5 is indeed found for the higher-resistivity material when carrier removal takes place. It is also seen from Fig. 21 that the correct value of K_0 can be computed from the values of L_0 and L_f for fluxes less than or equal to 1×10^{15} el/cm^2 and for resistivities below 100-Ω-cm. Since the same argument obviously holds for n-type material also, except that the η_c is an order of magnitude greater, the flux used for computing K_0 should be ten times smaller; i.e., 1×10^{14} el/cm^2 or less.

TABLE V

APPARENT SLOPE OF L VS. ϕ

ρ_i (Ω-cm)	K_0	η_c (cm^{-1})	APPARENT SLOPE
1	1.5×10^{-10}	0 0.05	0.5 0.5
10	9.33×10^{-11}	0 0.05 0.10	0.5 0.46 0.42
100	1.97×10^{-11}	0 0.05	0.50 –

The above criterion has been the basis of our method of finding K from the experimental data. Experimental measurements of the base resistivity before and after bombardment confirm the hypothesis that changes in base resistivity do occur. An estimate of η_c obtained from the surface-barrier cells on 1-Ω-cm, untreated n-type material is 0.1 cm^{-1}. The value is not exact since it was computed from the resistivity change without correcting for changes in carrier mobility.

The above development suggests why slope values less than 0.5 occur. The question arises why the slope values of the lithium-diffused cells are even lower than those of the phosphorus-diffused cells. One implication is that the base resistivity of the lithium-diffused cells has been increased, but this is not believed to occur. Alternatively, the presence of lithium either increases η_c or anneals some of the damage occurring during radiation. Either alternative would lead to a slope smaller than 0.5. The experimental data, which are incomplete and thus uncertain, indicate an increase in η_c in those cells containing lithium and, hence, a possible decrease in slope according to Fig. 21. A rough calculation of the effect of an annealing factor which is

proportional to the flux also predicts a decrease in slope at the higher fluxes. The correct interpretation of the small slope in the lithium-diffused cells obviously requires further experimental study.

D. CONCLUSIONS AND RECOMMENDATIONS FOR FUTURE WORK

Arguments can be made to extend even further the conclusions concerning lithium inferred from the experimental data. For example, in this study, the dependence of L_f and K on junction depth, which was found experimentally, may be due to the removal of lithium-rich material rather than a true dependence on junction depth as such. After all, the junction depth in several cases was not large enough to reduce the incident electron-energy significantly. Consequently, the base material should degrade in the same fashion as it does in the cells with a thinner junction. Furthermore, the specific ionization S_0 is found to be essentially the same in the cells with the deep, as well as the shallow, junctions. The same experimental arrangement should therefore give correct results for both types of cells.

Regardless of these arguments, however, it is concluded that the only unambiguous ways of demonstrating a defect interaction with lithium in this type of study are to study radiation damage in solar cells which have a uniform concentration of lithium in the base region and to study annealing of the radiation damage in control cells and cells containing lithium. Work on both of these programs is currently under way.

The following is a summary of the experimental study.

1. Al, B, Ga, In, and Gd are equivalent impurities as far as radiation resistance is concerned when they are used in solar cells with a base resistivity of 1 to 10-Ω-cm.
2. The radiation resistance of lithium-diffused cells with a deep junction exceeds that of phosphorus-diffused cells with a shallow junction.
3. The diffusion of lithium throughout n-type silicon reduces its resistivity, yet the radiation resistance of surface-barrier cells made from this material is higher than expected.
4. The slope of the L vs. ϕ data agrees more closely with theory for low-resistivity cells of both conductivity types than for high-resistivity and, in particular, lithium-diffused cells.
5. Of all the impurities studied so far, only the use of lithium has led to new and striking results. It seems reasonable that a fast diffuser like lithium would have a higher probability of interacting with radiation-induced defects than slow diffusers like B, Ga, In, Gd, and Al. Careful experimental evaluation of the dependence of L_f and K on both the base resistivity and junction depth must be made before such an interaction can reasonably be postulated.

III. STUDIES OF INTERACTION OF LITHIUM WITH DAMAGE CENTERS BY ELECTRON PARAMAGNETIC RESONANCE

A. INTRODUCTION

In this section we discuss the measurements of the interaction of lithium with radiation damage centers. While this might be included under the general heading of impurity interactions, it is being presented separately because the motivation and experimental techniques were somewhat different, and because the impurity and the defect studied have very special characteristics.

The work was begun in an attempt to measure directly the interaction between an impurity and a defect. While measurements of a parameter such as minority-carrier lifetime may be more appropriate for studying material or device properties, such measurements are essentially indirect in that they measure the *effects* of damage centers rather than their physical properties. Electron paramagnetic resonance measurements can measure changes in two of the most important properties of defects. These are charge state and density in the crystal. The charge state is important since it involves the outer electronic structure and hence the defect's electrical activity in the crystal. A direct measure of the defect density is very important because its changes with other experimental parameters can be charted.

For studies of impurity-defect interactions as described above, the impurity ideally should have the following properties. It should be easily and controllably introduced; it should be highly mobile (therefore interstitial); it should be a simple donor or acceptor (i.e., it should not cluster or be amphoteric); it should enter the crystal at sufficiently high concentrations at sufficiently low temperature; and, finally, it should be detectable by EPR measurements so that its behavior can be followed as it interacts with the defect. Two impurities which suggest themselves are lithium and copper. Copper has two disadvantages, however. It does not remain in a simple state in the crystal[29] (it exists both interstitially and substitutionally), and it does not have a measurable EPR absorption. Lithium on the other hand, after an initial period, remains a simple donor with a low ionization energy (0.033 eV)[30] which has a well-defined EPR line.[31] It has, in addition, all the desirable features listed above.

The defect we have initially chosen to study is the C-center[4] in n-type silicon rather than the A-center[4] – even though the A-center is thought to be the one that decreases the minority carrier lifetime in solar cells.[32,2] There are several reasons for this, most of which involve an EPR investigation of the center. The C-center is the dominant center at high electron energies and fluxes, supplanting the A-center in the EPR spectrum at energies above about 3 MeV.[33,2] The C-center is a primary, stable defect which does not anneal appreciably at temperatures up to 300°C.[33] The A-center, on the other hand, anneals readily at low temperatures ($\sim$ 60°C) and requires atomic movement for its formation.[2] One cannot produce high concentrations ($> 10^{16}/cm^3$)

of A-centers to the exclusion of all others. However, this might be done with the C-center. And, finally, since we expected to examine the damage centers under low power operation of the spin resonance spectrometer (see Section I-C), choosing the C-center would reduce or eliminate any sensitivity problems we may otherwise encounter in the instrumentation.

B. EXPERIMENTAL TECHNIQUES

The paramagnetic resonance spectrometer used was a Varian model V4500 heterodyne unit with a klystron frequency of about 9.1 Gc/sec. The magnetic field modulation operated at 100 kc/sec and had an amplitude at most one tenth the width of the resonance line studies. All measurements were made at liquid neon temperatures, 27°K, with the silicon samples placed with reproducible geometry in the microwave cavity. Input power levels were well below those at which the defect resonance lines saturate (see Section I-C).

The wafers to be measured were about 1 cm long and had a cross section of about 2 mm by 0.5 mm. They had been electron-irradiated at 6 MeV with fluxes varying from about 2×10^{16} el/cm^2 to about 4×10^{17} el/cm^2, and some of them had been used in the introduction rate measurements presented in Section I of this report. It was found that the EPR damage spectrum produced by such irradiations was altered only slightly by heat treatments up to 350°C. Since this temperature was the upper limit used for the introduction of lithium, some of the same wafers used for the introduction rate measurements were used for the lithium interaction measurements. Thus, the lithium is diffused into the wafers after they are irradiated and have ample opportunity to "move around" in the damaged lattice.

Lithium was introduced into the crystal by diffusion from a mineral oil suspension in a hydrogen ambient. The temperature determined the amount of lithium introduced. Excess lithium was removed from the surface and the wafer was then etched lightly to insure the elimination of surface states. The concentration of electrically active (donor) lithium was determined from resistivity measurements.

C. EXPERIMENTAL RESULTS

When one examines the EPR spectrum of n-type silicon which has been bombarded by 6-MeV electrons at high ($> 2 \times 10^{16}$ el/cm^2) fluxes, the dominant resonances observed are those of the C-center and, to a lesser extent, the E-center. Both their g-values are anisotropic and lie between 2.0005 and 2.0135.[4] They are invariably seen in dispersion mode representation. While there is some evidence indicating that we should be seeing primarily the C-center, the width of the damage resonance lines cannot rule out the possibility that E-centers are also present[33] in the EPR spectrum.* If lithium is present, its resonance line can be presented in either the

*The E-center is a phosphorus atom and a vacancy. It is characterized by a doublet structure with about a 10-gauss separation. We do not see this, probably because other resonances are obscuring it.

dispersion or the absorption mode. However, we have found that reproducible dispersion mode representation is very difficult due chiefly to difficulties in reproducing both the phasing and the degree of sample isolation in the microwave cavity. Accordingly, we will exhibit the lithium resonance in the easily reproducible absorption mode whose signal strength has been found to be the same (within about 20%) of the dispersion mode signal strength.

The lithium g-value is 1.9985.[31] We have not been able to detect the fine structure reported by Feher.[31] Unfortunately, the silicon conduction electron line ($g = 1.9987$)[31] is so closely situated to the lithium line that our spectrometer was not able to resolve the two when measured simultaneously. This has prevented our using the silicon conduction electron line as a calibrator for a particular EPR spectrum.

The base doping ($\sim 1 \times 10^{16}/cm^3$) of the n-type crystals is phosphorus. At low temperature and at low concentrations ($< 4 \times 10^{17}/cm^3$) its donor resonance has a doublet structure easily identifiable by its hyperfine separation of about 40 gauss.[34] It appears in our spectra in small concentrations ($\sim 10^{14}/cm^3$ to $10^{15}/cm^3$) consistent with Watkins' findings that electron irradiation sharply reduces the phosphorus resonance signal.[2]

Figure 22 shows three EPR spectra taken on (a) unirradiated silicon which has been diffused with lithium at 500°C, (b) unirradiated silicon which has been diffused with lithium at 300°C, and (c) silicon irradiated by a flux of 2×10^{16} el/cm^2 at 6 MeV prior to diffusing lithium into it at 300°C. The spectra show that for the 300°C lithium diffusion (for which the lithium content is about $3 \times 10^{16}/cm^3$) the electron irradiation has caused the disappearance of the ordinarily strong lithium resonance – leaving only a damage spectrum. A significant discrepancy is indicated here. The C-center introduction rate[2,33] is only between 0.005 and 0.01 cm^{-1}, so that the C-center concentration is about $10^{14}/cm^3$.* Yet the irradiation removes about $3 \times 10^{16}/cm^3$ paramagnetic lithiums. Since we know that A-centers and E-centers, among others, are produced at much higher introduction rates (~ 0.1 cm^{-1})[2] we conclude that many other defects are also present which can somehow affect paramagnetic lithium – we merely do not observe them in the resonance experiment.

If a new paramagnetic center were to appear when both lithium and defects are present, then this would furnish unambiguous proof that a new complex was being formed. Such, however, was not the case and our measurements must depend on *relative* changes in the magnitude of the lithium and defect resonances.

Figure 23 shows typical spectra of five irradiated silicon wafers. The wafers had the same orientation (111) and they all weighed between 22 and 24 mg. The first was irradiated with 1×10^{17} el/cm^2 and was then merely heat-treated for one hour at 350°C. The phosphorus doublet and the damage resonance lines are indicated. The second had lithium diffused into it at 325°C

*This number is approximately verified in several instances by the magnitude of the phosphorus doublet – see, for example, Fig. 23.

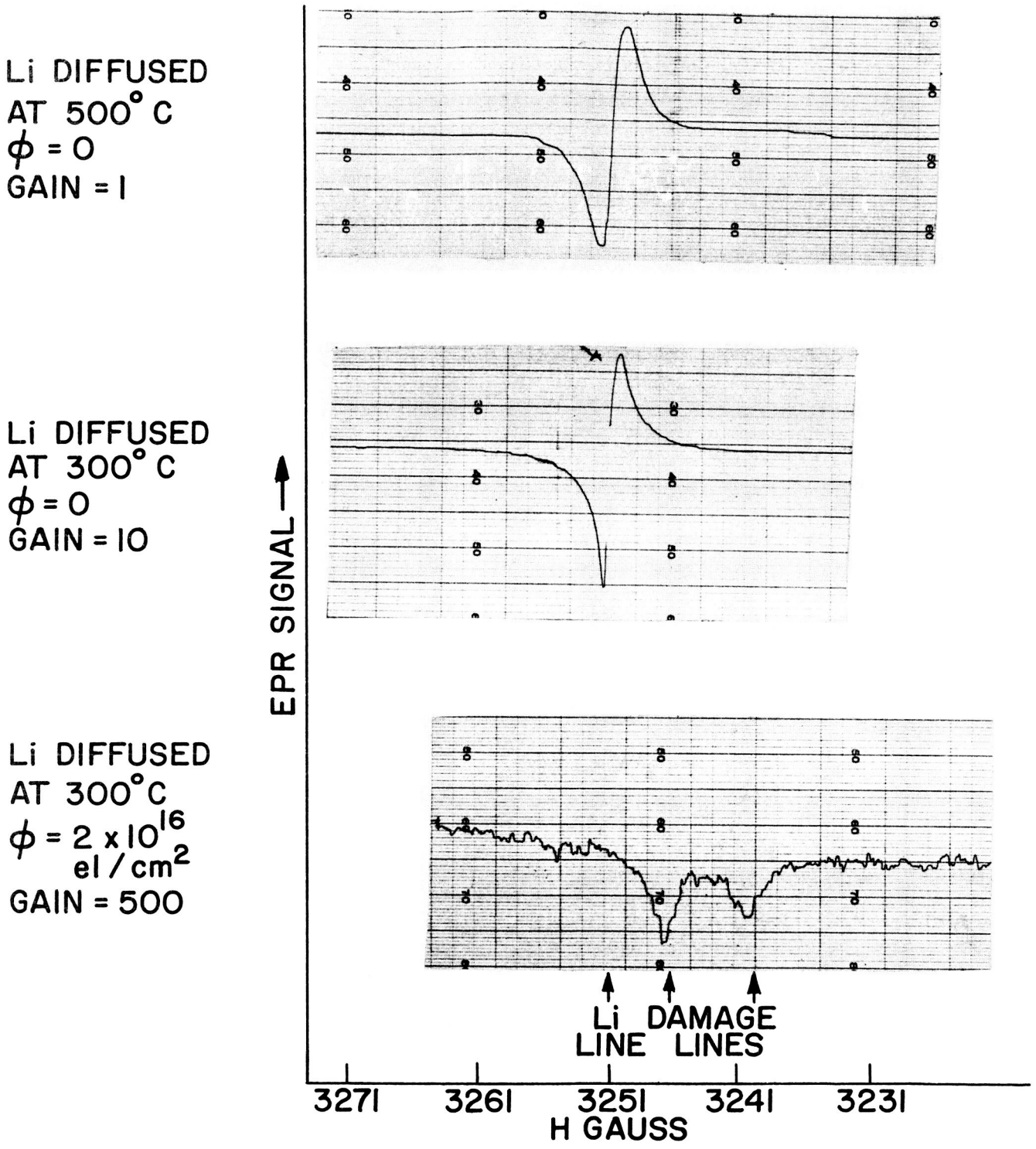

Fig. 22. EPR spectra showing effects of lithium content and irradiation on lithium resonance line.

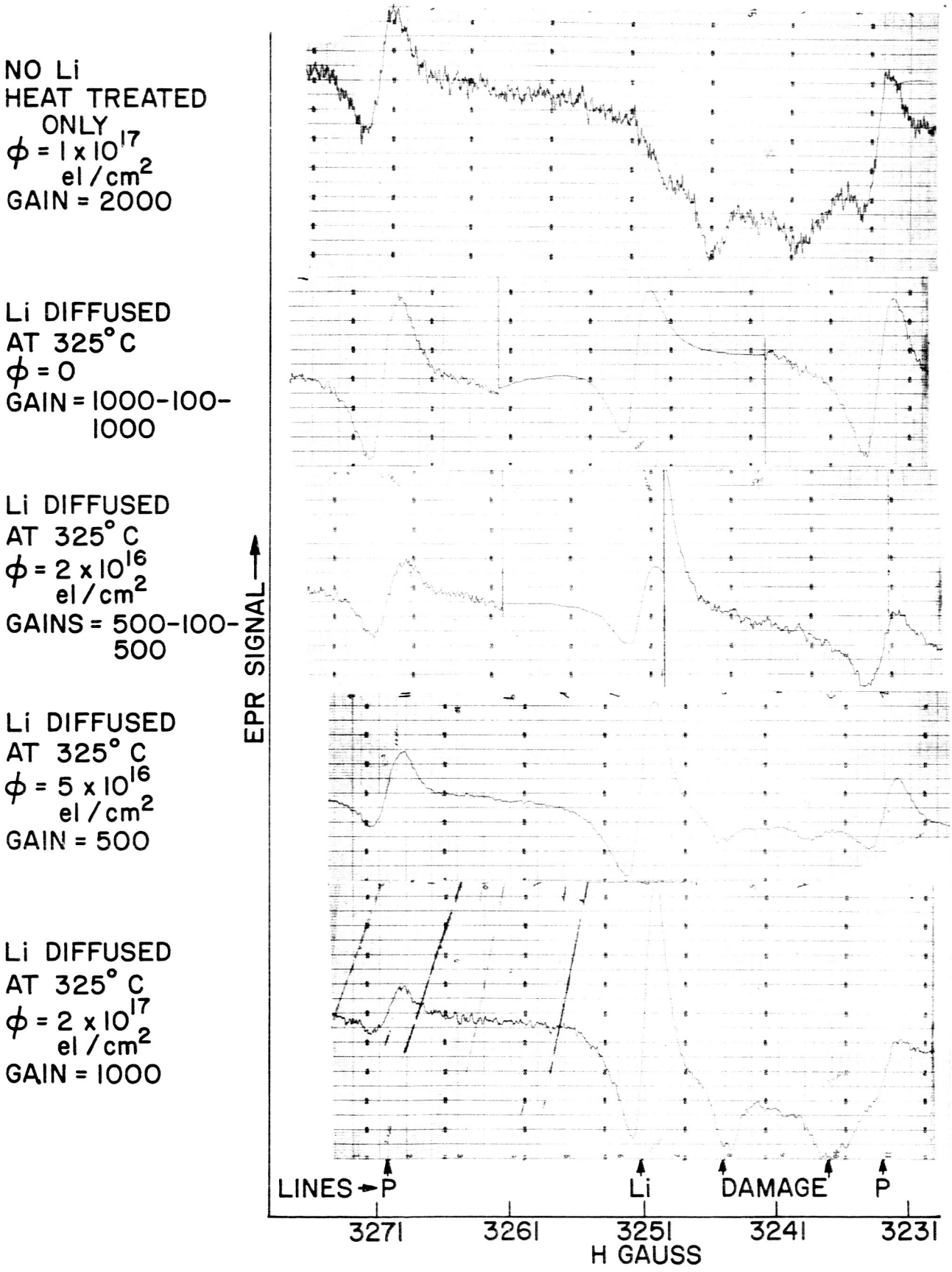

Fig. 23. EPR spectra showing decrease of lithium lines and growth of damage lines with irradiation.

and was not irradiated. The third, fourth, and fifth were irradiated with 2×10^{16}, 5×10^{16}, and 2×10^{17} el/cm^2, respectively, and then had lithium introduced at 325°C.* Note the change in gain settings for different parts of the spectrum. The decrease of the lithium line and the growth of the damage lines are clearly evident. In Fig. 24 we show three more spectra in which lithium has been introduced at 350°C (lithium concentration about 5×10^{16}/cm^3). Here, although no damage lines are seen, the lithium resonance nonetheless decreases as the irradiation dose increases. Note again the different gain settings. This again strongly suggests that defects other than C-centers, and in higher concentrations, are formed by the irradiations.

The reasons for the changes in the magnitude of the phosphorus doublet lines in two cases are not clearly understood. Their effect on the spectra can be eliminated without losing their useful function of serving as markers by using a *separate* piece of silicon with a known concentration of arsenic. Arsenic has an EPR quadruplet[34] structure with a known magnetic field position (hyperfine separation of about 70 gauss). In addition, the arsenic lines can themselves furnish calibrators for quantitative measurements of the damage and lithium lines.

Table VI summarizes the salient semiquantitative features of our EPR data in terms of the magnitudes of the lithium and damage lines. From it one can draw the principal conclusion that increasing the radiation dose causes a decrease in the lithium resonance regardless of whether the damage resonance is seen or not, and that the presence of, and increases in, the lithium concentration cause a decrease in the damage resonance.

TABLE VI

MAGNITUDES OF LITHIUM AND DEFECT RESONANCE SIGNALS (IN ARBITRARY UNITS) WITH VARIOUS FLUXES AND LITHIUM CONTENTS.

Flux (el/cm^2)	Li-Diffusion Temperature	Li Resonance Magnitude (Arbitrary Units)	Defect Resonance Magnitude (Arbitrary Units)
2×10^{17}	325°C	18	7.5
1×10^{17}	325°C	35	4
5×10^{16}	325°C	53	0 – 1
0	325°C	98	0
2×10^{17}	500°C	1300	0
2×10^{17}	350°C	60	0
2×10^{17}	325°C	18	7.5
2×10^{17}	300°C	0	14
2×10^{17}	--------	0	12
2×10^{17}	350°C	60	0
1×10^{17}	350°C	100	0
0	350°C	210	0

*This temperature had to be determined empirically. Earlier, 300°C was found to be too low. No lithium line was observed. A temperature of 350°C, however, was too high for these experiments, because no damage lines were observed.

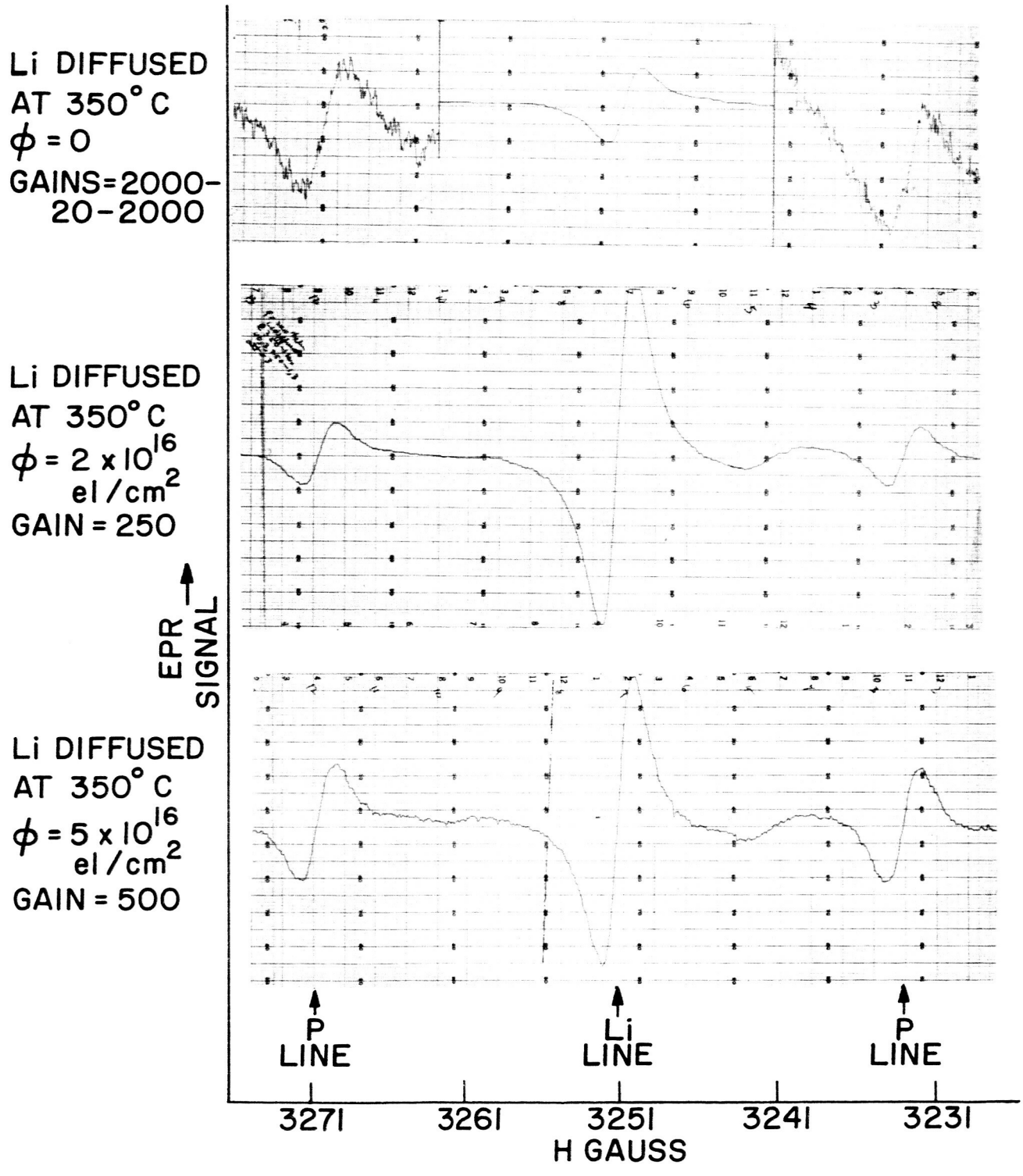

Fig. 24. EPR spectra showing effect of irradiation on lithium resonance line.

D. CONCLUSIONS AND RECOMMENDATIONS FOR FUTURE WORK

Two major conclusions can be drawn from this work which strongly indicate future courses of study. The first is that under all conditions in which damage spectra and/or lithium spectra can be unambiguously measured, there is always an increase in the one accompanied by a decrease in the other. Table VI shows this clearly. Whether the indicated interaction is one in which lithium actually forms a complex with the defect or one in which the lithium donor merely supplies an electron to an (damage level) acceptor is not clear, although the former is suggested by lithium's high atomic mobility. This result suggests that at least a part of the future work in this field be directed toward a specific answer to this question. This might be done, for example, by incorporating lithium into the crystal *before* electron irradiation and then heating it to successively higher temperatures (but not too high) while measuring EPR spectra after each heat treatment. Since this would not change the electrical nature of the shallow lithium donor, changes in the EPR spectra could then be ascribed to the atomic migration of the lithium. Of course, the "natural" annealing of the damage center during these treatments would have to be monitored during these experiments.

The second conclusion is that high-energy, high-flux electron irradiations are not the most appropriate conditions for a study of lithium-defect interactions. Diffusing lithium into the crystal at, for example, 300°C results in a lithium concentration of about $2 \times 10^{16}/cm^3$. Yet no lithium resonance is observed after an introduction of only about 10^{14} to 10^{15} C-centers. The very strong implication is that although only the C-center may have an observable resonance under these conditions, other defects may still have been formed. Indeed, the A-center and the E-center are formed with production rates between 10 and 100 times larger than that of the C-center. These other defects may still be present in the crystal but may simply be in the wrong charge state to have a resonance. Thus, while using high-flux, high-energy irradiations may insure a strong signal, they also inject an element of ambiguity into attempts at detailed analysis and interpretation. The indicated line of attack for this problem is to work at low energies (< 1.5 MeV) and low fluxes ($< 10^{16}$ el/cm^2). With these irradiations, according to defect production curves of Watkins,[2] only A-centers appear and grow linearly with flux while the base-doping resonance, e.g., phosphorus, concomitantly disappears at a similar rate. The changes in these resonances do not appear to be complicated by any other factor.

Singling out the A-center for this work, hopefully to the exclusion of other damage centers, may provide two more advantages. One is that, as mentioned earlier, it is believed that the A-center has been identified as the one which destroys the lifetime in n-type silicon.[35,2] If this is so, then impurity effects on lifetime degradation (including lithium) discussed in Section II, may be correlated with the lithium-defect interaction studied by EPR. The second is that working with only the A-center enhances what chance we might have of seeing a new paramagnetic center when lithium and defects are given a chance to form complexes. This would be the best evidence possible for the existence of lithium-defect interactions.

IV. SUMMARY OF LOW-ENERGY PROTON BOMBARDMENT OF Si AND GaAs SOLAR CELLS

The following results were obtained when silicon and GaAs cells were irradiated with 185- to 530-keV protons.

1. The short-circuit current I_{sc} of the GaAs cells degraded rapidly with flux ($\sim$ 35%/decade). Over most of the flux range, the degradation in open-circuit voltage V_{oc} was small, so that the drop in output power P_{out} was mostly due to the drop in I_{sc}.

2. In the silicon cells, V_{oc} fell rapidly with flux ($\sim$ 20%/decade). The value of I_{sc} changed little to a certain point, and then it fell rapidly with flux ($\sim$ 50%/decade). Consequently, the drop in V_{oc} contributed substantially to the drop in P_{out}.

3. At any given flux, the damage in either GaAs or silicon cells increased as the proton energy increased.

A self-consistent model which explains these results was developed as follows. For efficient operation, GaAs cells require collection of photogenerated carriers from surface regions of the cell, while silicon cells depend upon collection from the base region. The short range of 185- to 530-keV protons results in damaged regions up to 6.8 μ deep in silicon and 3.5 μ in GaAs, i.e., primarily the surface region of the cells. Hence, the cell properties which will be most affected by radiation are carrier collection in the GaAs and junction rectification in the silicon cells. The effectiveness of the higher-energy protons in producing cell degradation arises from their ability to penetrate the material further, damaging more of the volume from which carrier collection occurs. An adequate formulation of the spectral response was developed. This mathematical description exhibits qualitatively those features found experimentally.

A more detailed treatment of this material can be found in the First Semiannual Report prepared under this Contract in May, 1964.

REFERENCES

1. G. Bemski, J. Appl. Phys. **30**, 1195 (1959).
2. G. D. Watkins, J. W. Corbett and R. M. Walker, J. Appl. Phys. **30**, 1198 (1959).
3. G. D. Watkins and J. W. Corbett, Phys. Rev. **121**, 1001 (1961).
4. G. D. Watkins and J. W. Corbett, Faraday Soc. **31**, 86 (1961).
5. G. D. Watkins, International Conference on Semiconductors, Paris, (1964).
6. A. M. Portis, Phys. Rev. **91**, 1071 (1953).
7. M. Weger, Bell. Syst. Tech. J. **39**, 1013 (1960).
8. G. D. Watkins and J. W. Corbett – To be published.
9. G. E. Poke, "Paramagnetic Resonance," W. A. Benjamin, Inc., New York City (1962).
10. D. E. Hill, Phys. Rev. **114**, 1414 (1959).
11. Space Technology Laboratories, Interim Report MR-32, "Electron Energy Dependence of Radiation Damage in Silicon Solar Cells," Contract No. NAS 5-1851, July 1964.
12. V. S. Vavilov and A. E. Plotnikoff, J. Phys. Soc. Japan **18**, 230 (1963).
13. J. Baicker and B. Faughnan, J. Appl. Phys. **33**, 3271 (1962).
14. G. Wertheim and D. Buchanan, J. Appl. Phys. **30**, 1232 (1959).
15. G. Watkins, Bull. Am. Phys. Soc. **9**, 48 (1964).
16. Tkachev, Plotnikov and Vavilov, Sov. Phys. Solid State **5**, 2333 (1964).
17. J. Mandelkorn, et al., J. Appl. Phys. **35**, 2258 (1964).
18. W. Rosenzweig, Bell Syst. Tech. J. **41**, 1573 (1962).
19. J. Loferski and P. Rappaport, J. Appl. Phys. **30**, 1181 (1959).
20. V. Linnenbom, NRL Report 5828, Sept. 28, 1962.
21. L. Spencer, Phys. Rev. **98**, 1597 (1955).
22. K. McKay and K. McAfee, Phys. Rev. **91**, 1079 (1953).
23. K. A. Wright and J. G. Trump, J. Appl. Phys. **33**, 687 (1962).
24. E. Wurst and E. Borneman, J. Appl. Phys. **28**, 235 (1957).
25. N. Hansen, IRE Trans. Nuc. Sci. **NS-9**, 217 (1962).
26. R. Sternheimer, Rev. Sci. Inst. **25**, 1070 (1954).
27. L. Katz and A. Penfold, Rev. Mod. Phys. **24**, 28 (1952).
28. R. L. Novak, Personal Communication.
29. C. B. Collins and R. O. Carlson, Phys. Rev. **108**, 1409 (1957).
30. C. S. Fuller and J. A. Ditzenberger, Phys. Rev. **91**, 193 (1953).

REFERENCES (Continued)

31. G. Feher, Phys. Rev. **114**, 1219 (1959).
32. G. K. Wertheim, J. Appl. Phys. **30**, 1166 (1959).
33. G. Bemski and B. Szymanski, J. Phys. Chem. Solids **24**, 1 (1963).
34. R. C. Fletcher, et al., Phys. Rev. **94**, 1392 (1954).
35. G. K. Wertheim, Phys. Rev. **105**, 1730 (1957).